Variable branching characteristics of peripheral taste neurons indicates differential convergence

Abbreviated title: Variation in Taste Neuron Morphology

Tao Huang[1]*, Lisa C. Ohman[1]*, Anna V. Clements[1], Zachary D. Whiddon[1], and Robin F. Krimm[1#]

[1]Department of Anatomical Sciences and Neurobiology, University of Louisville School of Medicine, Louisville, KY 40202

*These authors contributed equally to this work

[#]Correspondence to: Dr. Robin Krimm, robin.krimm@louisville.edu, MDR building, room 405B, 511 S. Floyd Street, Louisville, KY 40202

Key Words: taste, geniculate neuron, morphology, afferent, tongue

Classification: Biological Sciences

Number of pages: 37
Number. of Figures: 9
Number of Tables: 0
Number of multimedia files:4
Number of words in abstract: 228
Number of words in introduction: 640
Number of words in discussion: 1449

Acknowledgements: We would like to thank Chad Samuelsen for his help with cluster analysis and comments on the manuscript. We would like to thank Kaytee Horn for her help breeding and genotyping the mice and additional technical assistance. This project was supported by R21 DC014857 and R01 DC007176 to R.F.K and F31 DC017660 to L.O.

Authors declare no competing interests

ABSTRACT

Taste neurons are functionally and genetically diverse, but their morphological diversity remains completely unexplored. Using sparce cell genetic labeling, we provide the first reconstructions of peripheral taste neurons. The branching characteristics across 96 taste neurons show surprising diversity in their complexities. Individual neurons had 1 to 17 separate terminal arbors entering between 1 to 7 taste buds, of which 18 neurons also innervated non-taste epithelia. Cluster analysis separated the neurons into four groups according to branch complexity. The primary difference between clusters was the amount of nerve fiber within the taste bud available to contact receptors cells, which implies variation in the number of receptor cells providing input across neurons. Consistently, we found that the maximum number of taste receptor cells capable of providing convergent input onto individual gustatory neurons varied with a range of 1-22 receptor cells. Thus, differences in branching characteristics across neurons indicate that some neurons likely receive input from a larger number of receptor cells than other neurons (differential convergence). By dividing neurons into two groups based on the type of receptor cell most contacted, we found that neurons contacting primarily sour transducing receptor cells were more heavily branched than those contacting primarily sweet/bitter transducing taste receptor cells. This suggests that neuron morphology differs across functional taste quality. However, the considerable remaining variability within each group suggests differential convergence within each functional taste quality.

Authors declare no competing interests

Introduction

The chemical information from food is detected by taste receptor cells in the tongue and carried to the brain by sensory neurons. This chemical information includes taste qualities described as sweet, salty, sour, bitter, and umami (Contreras and Lundy 2000, Spector and Travers 2005, Yarmolinsky, Zuker et al. 2009, Carleton, Accolla et al. 2010, Ohla, Yoshida et al. 2019) as well as those that are not easily classified (Bachmanov, Tordoff et al. 1996, Tordoff 2001, Liu, Archer et al. 2016, Tordoff 2017, Lim and Pullicin 2019). Moreover, taste stimuli vary in intensity, and differences in stimulus intensity impacts quality coding (Ganchrow and Erickson 1970, Wu, Dvoryanchikov et al. 2015). Adding to their functional diversity, taste neurons respond to and are modulated by somatosensory stimuli (Lundy and Contreras 1997, Breza, Curtis et al. 2006, Yokota and Bradley 2016, Yokota and Bradley 2017). While numerous studies have focused on the functional diversity of this population of neurons, only recently has there been confirmation of their genetic diversity (Dvoryanchikov, Hernandez et al. 2017, Zhang, Jin et al. 2019). However, their morphological diversity remains completely unexplored.

Unlike the sensory neurons of skin (Maksimovic, Nakatani et al. 2014, Castillo, Diaz-Franulic et al. 2018), taste neurons do not participate in transduction (Chandrashekar, Hoon et al. 2006). Therefore, functional differences between gustatory neurons are thought to be determined entirely by the type of receptor cell they innervate (Yarmolinsky, Zuker et al. 2009). Consistent with this hypothesis, retrograde tracing studies conclude that most taste neurons innervate only a single taste bud (Zaidi and Whitehead 2006). In addition, functional studies conclude that limited convergence is required for quality coding at mid-range stimulus concentrations (Yoshida, Yasumatsu et al. 2006). Thus, despite the functional and genetic diversity of taste neurons, anatomical variation in these neurons was not expected, and was difficult to measure.

Authors declare no competing interests

A definitive measure of morphological diversity necessitates full reconstruction of the peripheral axon of individual neurons. However, anatomical tracers do not travel the full length of peripheral taste axons. Genetic labeling provides a practical alternative (Wu, Williams et al. 2012, Bai, Lehnert et al. 2015, Kuehn, Meltzer et al. 2019); however, obstacles to this approach also exist. First, the number of taste neurons innervating the tongue is miniscule relative to the somatosensory innervation of lingual epithelium. Thus, if neurons from both populations are labeled, individual taste axons will be indistinguishable from somatosensory axons. As these two populations of neurons express many of the same factors, the majority of genetic labels used in other systems are impractical for reconstructing taste neurons (Wu, Williams et al. 2012). Lastly, the tongue is an unusually dense tissue requiring relatively thin sections for antibody labeling, which renders full neuron reconstruction unusually tedious.

It is important to overcome these practical limitations to fully reconstruct the axonal arbors of taste neurons for several reasons. Classification of morphological diversity can be combined with molecular expression data to correlate morphologies with distinct functions (Abraira and Ginty 2013). Knowing whether or not morphological differences are present dictates whether this direction of inquiry would be informative for the field of taste. Furthermore, the degree of branching likely reflects the degree of connectivity with taste receptor cells (Chklovskii 2004), which would indicate that gustatory neuron responses are determined by both the type and number of receptor cells providing input.

In the present study, we used genetically directed sparse-cell labeling to fully reconstruct the complete peripheral morphologies of 96 neurons innervating taste buds in the tongue. Quantitative analyses revealed a surprising degree of diversity between taste neurons that, on average, innervate more taste buds than previously estimated. We demonstrate that neurons with more complex axonal arbors contact a large number of taste receptor cells, whereas those with simple endings contact only a few receptor cells. We conclude that individual neurons likely receive differing amounts of convergent information from taste receptor cells.

Authors declare no competing interests

MATERIALS AND METHODS

Animals

TrkB^{CreER} mice (*Ntrk2*$^{tm3.1(cre/ERT2)Ddg}$;, https://www.jax.org/ ISMR Cat# JAX:027214, RRID:IMSR_JAX:027214) were crossed with Cre-dependent AP mice (https://www.jax.org/; IMSR Cat# JAX:009253, RRID:IMSR_JAX:009253) to obtain *TrkB*^{CreER}:AP mice, or with Cre-dependent tdTomato mice ((Rutlin, Ho et al. 2014) https://www.jax.org/ RRID: IMSR_JAX:007914) to obtain *TrkB*^{CreER}:tdTomato mice. In these mice, either the reporter gene AP or tdTomato is expressed following TrkB-driven Cre-mediated gene recombination.

Fungiform taste buds decrease in number postnatally (Liebl, Mbiene et al. 1999, Patel and Krimm 2012), such that varying the experimental age of examination could introduce variation in fiber morphology. To avoid this potential confounding variable, all fibers were reconstructed in mice at postnatal day 60–62. Although all animals were examined at the same age, 27 *TrkB*^{CreER}:AP mice were injected with tamoxifen (0.5mg-1.0mg) at P40, those axons were reconstructed from 17 mice (8 male and 9 female), while 10 either had no labeled axons or too many labeled axons to reconstruct. To select from all neurons expressing TrkB during development, 48 pregnant dams were injected with 4 hydroxy tamoxifen at E15.5, 26 litters survived through birth, producing 21 mice (9 male an 12 female) that were of the correct genotype and had the correct number of axons that permitted reconstruction (1-4), 115 mice either had 0 labeled axons or too many to accurately reconstruct. In order to label one single tdTomato-positive axon in the tongue, 94 *TrkB*^{CreER}:tdTomato mice were injected with tamoxifen (0.3mg-1mg), producing a total of 21 half tongues with one labeled axon, while the remaining 167 tongue halves were determined to have either no labeled axons or too many (more than one) following serial sectioning of the tongue muscle. All animals were cared for in accordance with the guidelines set by the U.S. Public Health Service Policy on the Humane Care and Use of Laboratory Animals and the NIH Guide for the Care and Use of Laboratory Animals.

Authors declare no competing interests

Tamoxifen injections

Tamoxifen (T-5648, Sigma, St. Louis, MO) was dissolved in corn oil (C-8267, Sigma, St. Louis, MO) at 20 mg/ml by shaking and heating at 42°C. For embryonic injections, 4-Hydroxytamoxifen (4-HOT) (H-7904, Sigma, St. Louis, MO), the active metabolite of tamoxifen, was injected intraperitoneally into pregnant dams at E15.5. 4-HOT was prepared and injected as previously reported (Wu, Williams et al. 2012). Briefly, 4-HOT was dissolved in ethanol at 20 mg/ml by shaking and incubating at 37°C for 15 min and then stored at -20°C. Before use, the stock solution was dissolved in sunflower seed oil to a final concentration of 10 mg/ml 4-HOT, and the ethanol was evaporated by centrifugation under vacuum.

Alkaline phosphatase staining

Mouse tongues were dissected following perfusion with PBS containing 2% paraformaldehyde (PFA), 0.5% glutaraldehyde, and 2 mM $MgCl_2$. The tongues were cut in half and postfixed for 2 h. After rinsing twice in PBS with 2 mM $MgCl_2$, the tissues were transferred to PBS without $MgCl_2$, and incubated at 65°C for 2 h to inactivate endogenous AP. Then, the tongues were frozen in O.C.T. (Sakura Finetek, USA) and stored at -80°C before serial sectioning at 180 µm. The staining was performed according to a previous publication with slight modification (Badea, Wang et al. 2003). Briefly, the tongue sections were washed in 0.1 M Tris-HCl (pH 7.5) followed by 0.1 M Tris-HCl (pH 9.5) before incubating overnight at room temperature in 0.1 M Tris-HCl (pH 9.5) containing nitroblue tetrazolium and 5-bromo-4-chloro-3-indolyl-phosphate at the recommended concentrations (Vector Laboratories). After washing in PBS and postfixing in 4% PFA, the stained tissues were dehydrated with an ethanol series and cleared and mounted with 2:1 benzyl benzoate/benzyl alcohol (Sigma); sections were coverslipped with DPX (VWR).

Chorda tympani nerve transection

Mice were sedated with a 0.32-mg/kg intramuscular injection of medetomidine hydrochloride (Domitor) and anesthetized with 40 mg/kg ketamine hydrochloride (Ketaset). Mice were placed in a nontraumatic head holder to provide access to the nerve in the neck via a ventral approach (Guagliardo and Hill 2007). The chorda tympani nerve was located as it bifurcates from the lingual branch of the trigeminal nerve and was transected (portion was removed) without damaging the trigeminal nerve. The wound was sutured, and mice recovered on a water-circulating heating pad before being returned to their home cages. Atipamezole hydrochloride (2 mg/kg) was injected intramuscularly immediately after surgery to promote the reversal of anesthesia and thus reduce recovery time. Meloxicam was also administered orally through food pellets for 2 days after surgery; to achieve a dose of 1–2 mg/kg, 0.5 cc of a 0.5 mg/ml meloxicam solution was applied to each of two food pellets, which were then moistened with water and placed in the home cage. After 7 days, mice were euthanized and perfused with 4% PFA.

Fluorescent anterograde nerve labeling

The procedures used to label the chorda tympani with fluorescent tracers were previously described (Sun, Dayal et al. 2015). Briefly, adult *TrkB*^{CreER}:tdTomato mice, which had been given 4.0 mg tamoxifen via gavage for 3 weeks, were anesthetized and placed in the head holder as described above. A water-circulating heating pad was used to maintain body temperature. The chorda tympani nerves within the right tympanic bulla were cut near and peripheral to the geniculate ganglion, and crystals of 3 kDa fluorescein dextran (D3306; Invitrogen) were applied to the proximal cut end of the chorda tympani. A small amount of Kwik-Sil (World Precision Instruments, Inc., Sarasota, FL) was then placed over the cut ends of the nerves to prevent crystals from diffusing from the intended labeling site. Postsurgical treatment was the same as described above. After 24 h, mice were euthanized and perfused with 4% PFA. The geniculate ganglia were dissected and immediately mounted and imaged by confocal microscopy.

Immunohistochemistry

Mice were sacrificed by avertin overdose (4 mg/kg) and perfused transcardially with 4% PFA. Dissected tissues were postfixed in 4% PFA for 2 h (for thin serial sections) or overnight (thick sections and whole mounts), rinsed with PBS, and transferred to 30% sucrose at 4°C overnight. A razor blade was used to remove the circumvallate papilla; the tongues were then carefully split down the midline with a razor blade under a dissection microscope. Tongues were frozen the next day in OCT and stored at -80°C before sectioning on a cryostat or processing for whole-mount staining. To determine if tongue halves are innervated by a single fiber, the muscle at the base of the midline was isolated using a razor blade, frozen in OCT, and serially sectioned (30 µm) on the cryostat. Serial sections were thaw mounted onto slides in order and then cover slipped with Fluoromount-G (SouthernBiotech, Birmingham, AL). Sections were examined under a fluorescence microscope to determine how many labeled fibers enter the tongue.

To visualize taste buds and their innervation in serial sagittal sections, each tongue half was sectioned sagittally from the midline to the lateral edge at 90 µm. Each section was processed in its own well, so that the section order was maintained. Floating sections were blocked at 4°C in 0.1 M PB with 3% donkey serum and 0.5% Triton X-100 overnight and then incubated for 5 days at 4°C with primary antibodies, rabbit anti-DsRed (1:500, RRID:AB_632496, Living Colors DsRed polyclonal; Takara Bio USA) and rat monoclonal anti-Troma1 (1:50, RRID:AB_531826; Developmental Studies Hybridoma Bank, Iowa City, IA). Sections were then rinsed four times for 15 min each, incubated for 2 days in secondary antibodies, Alexa 488 anti-rat IgG (1:500; Jackson ImmunoResearch Labs Cat# 712-545-153, RRID:AB_2340684) and Alexa 555 anti-rabbit IgG (1:500;Molecular Probes Cat# A-31572, RRID:AB_162543), rinsed another four times for 15 min each, and then mounted and coverslipped.

Whole-mount immunohistochemistry of the lingual epithelium was performed to visualize the innervated taste buds. First, the underlying muscle and lamina propria were removed as described previously (Ohman-Gault, Huang et al. 2017). The isolated lingual epithelium was then

washed for 15 min (3 times) in 0.1 M PB. Tissues were then incubated in blocking solution (3% donkey serum, 0.5% Triton X-100 in 0.1 M PB) at 4°C overnight and then incubated for 5 days at 4°C with primary antibodies (PLCβ2, 1:500, RRID:AB_2630573; Santa Cruz Biotechnology) in antibody solution (0.5% Triton X-100 in 0.1 M PB). Tissues were rinsed four times for 15 min each with 0.1 M PB, incubated with secondary antibodies (1:500, Alexa Fluor 488 AffiniPure, RRID:AB_2340619; Jackson ImmunoResearch), rinsed again (4 times for 15 min each with 0.1 M PB), and then incubated with 5% normal rabbit serum in antibody solution. Tissues were then rinsed and incubated with AffiniPure Fab fragment donkey anti-rabbit IgG (20 µg/mL, RRID:AB_2340587; Jackson ImmunoResearch) in antibody solution, rinsed, and incubated with Zenon Alexa Fluor 555 rabbit IgG labeling kit (according to the instructions for Zenon complex formation [Z25305; Invitrogen]) using anti-DsRed (1:500; RRID:AB_10013483; Living Colors DsRed polyclonal; Takara Bio USA). Tissues were rinsed, incubated for 5 days at 4°C with Car4 primary antibody (1:500, RRID:AB_10013483; R&D Systems), rinsed, and then incubated with secondary antibodies (1:500, Alexa Fluor 647 AffiniPure, RRID:AB_2340438). Tissues were then rinsed again, mounted with Fluoromount-G, and coverslipped (high precision, 0107242; Marienfeld).

Confocal Imaging

Taste bud images were obtained using an Olympus Fluoview FV1000 confocal laser-scanning microscope with a 60× lens objective using a zoom of 3, Kalman 2. Image sizes were initially set at 1,024 × 1,024 pixels but were cropped to reduce scanning time and bleaching. Serial optical sections at intervals of 0.47 µm in the Z dimension were captured, which is the optimal size at ×60 magnification for 3D reconstruction. All colors were imaged sequentially in separate channels to avoid bleed through. Image stacks were then deconvolved using AutoQuant X3 software (Media Cybernetics, Maryland) to reduce out-of-focus florescence and improve image quality.

Experimental Design and Statistical Analyses

Image analysis

AP-stained taste axons were reconstructed under a microscope (using a 60× lens objective with a 2-mm working distance and numerical aperture of 1.0) using Neurolucida software (MBF Bioscience). The axons were reconstructed from the areas where the axons enter the tongue to all terminal ends. The tongue outline was reconstructed by using Neurolucida and Photoshop software (Adobe). Individual arbors innervating whole immunostained taste buds were also reconstructed from confocal image stacks using Neurolucida software. Reconstructions were then analyzed using Neurolucida Explorer (MBF Bioscience).

Imaris software version 6.4.2 (Bitplane) was used to generate the 3D reconstructions and to measure proximity of nerve arbors to receptor cells. The colocalization function in Imaris was not used, because it contains many user-selected options that might contribute experimenter bias. More importantly, it was unclear how much colocalization there would be between labels in two separate cell types: the receptor cells and nerve arbors. Also, the physical relationship between any two florescent markers in a sample is influenced by tissue processing, intensity and wavelength of labels, the location of the labeled protein in the cells, deconvolution, orientation of the tissue, etc. Thus, the physical distance between nerve arbors and receptor cells (proximity) was measured with a distance transformation function in Imaris, which was previously described (Valm, Cohen et al. 2017). This algorithm permits identification of an object and then its distance from any/all other objects in a defined 3D space. This was accomplished using automated thresholding, which identified the surface of labeled objects (cells and nerve arbors) and then determined the distance between them in voxel increments. Thresholds were automatically generated with no input from the operator to limit bias. Because the sampling was at roughly twice the resolution of the microscope, distances of two voxels or less are equivalent to the colocalization artifacts that occur when two objects of different colors are sufficiently close

(Corson and Erisir 2013, Stratford, Larson et al. 2017). However, the proximity analysis enables the distance between any two cells to be measured.

To display the relationship between a single arbor and receptor cell, individual taste receptor cells and terminal arbors were segmented in Imaris, and the fluorescent channel was only duplicated within the selected region. Segmentation was completed after analysis for illustrative purposes only.

Data analysis.

Sixteen different anatomical measures were used in the k-means cluster analysis to group neurons on the basis of similarity: age of the animal at the time of tamoxifen injection, number of taste buds innervated, total length of the peripheral axon, location of the tongue innervated, number of branch points below the epithelium, number of branch points in the taste bud, total number of branch ends, number of branch ends per taste bud, mean terminal branch length, combined terminal branch length, combined terminal arbor length, number of terminal arbors, number of widened endings, number of non-taste endings, distance from the base of the tongue to the first branch point, and highest branch order. Cluster analysis was performed using MATLAB (https://www.mathworks.com/help/stats/k-means-clustering.html?s_tid=srchtitle). Time of tamoxifen injection and sex of the animals were compared using 2 (groups) X 16 (measures) ANOVA*s*. Characteristics were compared across clusters by first testing whether the measure was normally distributed across all 4 clusters using the Shapiro-Wilk test. If the measure was normally distributed, then differences were determined using a one-way analysis of variance with a Tukey's *post hoc* analysis. If they were not normally distributed differences across multiple groups were compared using a Kruskal-Wallis test, while two groups were compared using a Mann-Whitney test. Multiple comparisons were avoided by comparing a limited number of factors relevant to the study. However, when more than one comparison was made for a measure a Bonferroni's correction factor was used. Pearson product-moment correlations were used to

analyze the relationship between variables. The alpha level was set at $P<0.05$, and actual P values are reported.

Results

Genetically directed sparse labeling of taste neurons.

Taste neurons are functionally and genetically diverse, but it is unclear whether there is any morphological diversity within this population of neurons. To evaluate morphological diversity, we used an inducible genetic technique that primarily labels taste neurons, and not the more abundant somatosensory neurons that innervate the tongue epithelium. The neurotrophin receptor TrkB is expressed in most taste neurons within the geniculate ganglion (Huang and Krimm 2010, Tang, Rios-Pilier et al. 2017, Rios-Pilier and Krimm 2019), but very few TrkB-positive trigeminal neurons innervate the tongue (Wu, Arris et al. 2018). Therefore, we used TrkB^{CreER}:alkaline phosphatase (AP) mice to reconstruct single taste nerve axons innervating the tongue (Rutlin, Ho et al. 2014). AP has been used to reconstruct single axonal arbors of somatosensory neurons (Badea, Williams et al. 2012, Wu, Williams et al. 2012), and it has the advantage of being stained with adequate intensity to be visualized in thick tissues, allowing the stained axons to be more readily reconstructed than with fluorescent labeling.

We injected 27 postnatal day 40 *TrkB*^{CreER}:AP mice with low doses of tamoxifen to label a small number of individual neurons by adulthood (postnatal day 60) and reconstructed the peripheral axons from where the chorda-lingual nerve entered the tongue to where they terminated at the epithelial surface (Fig. 1A and B). The number of neurons labeled was variable and not strictly dose dependent. When more than four axons were labeled, they crossed paths, making it impossible to follow individual axons. However, at the same doses some tongues did not contain even a single quantifiable axon. We reconstructed a total of 41 quantifiable neurons from 17 animals.

Authors declare no competing interests

Since TrkB expression decreases in the geniculate ganglion after embryonic day 15.5 (E15.5) (Rios-Pilier and Krimm 2019), we were concerned that injections at postnatal day 40 did not include the full population of taste neurons. Therefore, we injected *TrkB*^{CreER}:tdTomato mice with a high dose of tamoxifen (4mg/day for two weeks) to capture as many TrkB-expressing neurons as possible and then labeled the taste neurons projecting to the tongue with a fluorescent tracer (Sun, Dayal et al. 2015). We found that 73% (n=2, 71%, 75%) of tongue-innervating geniculate ganglion neurons were tdTomato positive. Thus, the majority of TrkB-expressing taste neurons are labeled when adults are injected with tamoxifen (Rios-Pilier and Krimm 2019). Nevertheless, to circumvent the reduction of TrkB during development, we injected 58 pregnant dams (at E15.5) with 0.5, 0.75, or 1.0 mg 4-Hydroxytamoxifen. A total of 55 axons were reconstructed from 21 mice injected at E15.5.

All reconstructed axons were from tongues of adult mice (postnatal day 60–62) regardless of the age at injection. The age at time of tamoxifen injection P40 (n=41) and E15.5 (n=55) had no significant effect on the measured morphological characteristics (16 measures, listed in methods) of the reconstructed axons ($F_{(1, 15)} = 3.1$, $P = 0.08$;ANOVA). In addition, there were no differences in the morphological characteristics of axons reconstructed from male (n=45) and female (n=51) mice ($F_{(1, 15)} = 0.91$, $P = 0.07$:ANOVA). Therefore, we combined these data to yield a total of 96 fully reconstructed peripheral taste nerve axons (available to the research community at neuromorpho.org/dableFiles/tao_krimm/Supplementary/Tao_Krimm.zip). Across these neurons, we observed that individual axons had branch points in the tongue muscle, lamina propria, and epithelium (Fig. 1C). Branch points outside the taste bud dictated the number of separate terminal arbors, the portion of the axon innervating taste buds (range, 1–17 per neuron), whereas branch points inside the taste bud dictated the variation in complexity of these different terminal arbors.

The large number of branch points in the musculature and lamina propria was surprising, because in mice most taste neurons are thought to innervate only a single taste bud (Zaidi and Whitehead 2006). When one tracer was injected into a single taste papilla and another was injected into the surrounding papillae there were few double-labeled neurons (Zaidi and Whitehead 2006, Zaidi, Krimm et al. 2007), indicating minimal branching outside of the taste bud. Because these earlier studies assumed that gustatory neurons innervate adjacent taste buds, we examined heavily branched neurons to determine if they always innervated adjacent papillae. Many neurons innervate immediately adjacent papillae. However, we also found some taste neurons innervating multiple taste buds that were not located in the adjacent fungiform papillae in the tongue (Fig. 2A). Unfortunately, because sections were thick and tissue other than nerve fibers were unstained, it was not possible to evaluate the number of times this occurred. Another explanation for why these findings differ from estimates in the literature is that single small arbors may not take up sufficient quantities of tracer to visible at the cell body. To see if this was likely, we determined the frequency that individual neurons only innervate individual taste buds with a single arbor, and found this to be the vast majority (Fig. 2B). Therefore, we conclude that reconstructions of individual arbors provide a more accurate representation of branching characteristics and number of taste buds innervated than tracer injections.

In the 38 tongues from which the 96 TrkB-positive axons innervating taste buds were reconstructed, we also observed 4 labeled axons that did not innervate taste buds. To determine if all labeled axons innervating the tongue were from the primary taste nerve innervating the front of the tongue (the chorda tympani nerve), we injected *TrkB*^{CreER}:tdTomato mice (*n*=2) with a high dose of tamoxifen to label many TrkB-positive neurons and then transected the chorda tympani nerve. The axons remaining in the tongue after degeneration of the chorda tympani nerve are from another (non-taste) source (Guagliardo and Hill 2007). Although the number of TrkB-positive axons entering the tongue on the sectioned side was reduced than on the contralateral side, some

TrkB-positive axons remained in the tongue (Fig. 2). These TrkB-positive axons innervating the tongue were likely from the trigeminal ganglion (Wu, Arris et al. 2018). To determine if these non-chorda tympani TrkB-positive axons innervate taste buds, we quantified TrkB-positive innervation in the taste buds. We found that 100% of taste buds were innervated by tdTomato-labeled nerve axons on the intact side of the tongue (Fig. 2), whereas only 5% of the taste buds were innervated by tdTomato-labeled nerve axons on the transected side. These innervated taste buds (four in two mice) were located at the midline ventral tongue tip where the mid-line is less clear, such that the innervation was likely from the contralateral chorda tympani nerve. We conclude that most TrkB-positive axons innervating the tongue are from the chorda tympani and that axons from other sources do not typically innervate taste buds. Therefore, nerve axons that did not innervate taste buds were not reconstructed or included in the data set, as their nerve of origin was uncertain.

Individual axons of taste neurons vary in branching characteristics.

Somatosensory neurons of the dorsal root ganglion can be classified as types by their distinct morphological endings in skin (Wu, Williams et al. 2012), this was not the case with taste neurons. However, we did observe that some taste axons branched very little to innervate a single taste bud, while others displayed extensive branching, with up to 17 separate terminal arbors innervating as many as 7 taste buds and 40 total branch ends. To organize these neurons into descriptive groups (clusters), we measured 16 separate morphological characteristics (see Methods) and performed a k-means clustering analysis (Fig. 4A and B). Silhouette values were used to estimate the optimal number of clusters. A four-cluster model provided the second highest mean silhouette value (0.6944) while having no negative values, an indication of miss-assignment. These four clusters represented a gradual increase in branch complexity (measured morphological characteristics related to branching), from the simplest in cluster 1 to the most complex in cluster 4. Each axon's highest branch order (with the axon entering the tongue being the first order and subsequent branching adding additional orders), number of total branch ends,

and combined terminal arbor length in the taste bud were the three characteristics allowing greatest separation between clusters (Fig. 4D). Just under half of the axons constituted cluster 1, representing the simplest branch complexity (Fig. 4B). The remaining half were of increasing complexity, with the fewest number in the most complex cluster (cluster 4). Total terminal arbor length in the taste bud provided the clearest separation of the clusters ($F_{(3,92)} = 368, P=0.001$; Fig. 4C and D [bottom]). This measure corresponds to the amount of the nerve fiber (axon) available to contact taste receptor cells. This finding implies that number and not just type of receptor cells providing input to taste neurons varies across the taste neuron population.

Nearly half (44%) of taste axons have simple peripheral morphologies.

Representative examples of the simple morphologies of two cluster 1 neurons are shown in Figure 5A and B, which innervated one and two taste buds, respectively. Terminal arbors (the portion of the axon terminating into the taste bud) of cluster 1 neurons typically had two (Fig. 5A) to three (Fig. 5B, second taste bud) branch points within the taste bud. Many terminal arbors branched within the taste bud, with only a single branch point and two branch ends. Most of the axons in cluster 1 neurons innervated one or two taste buds (81%; Fig. 5C), with only one to two terminal arbors (Fig. 5D). The number of taste buds that are innervated corelates with the total length of the axon (r=0.64, *P*=0.00000671, Fig. 5D). A smaller proportion (19%) of the cluster 1 axons innervated three or more taste buds (Figure 5C) with four or more separate terminal arbors (Fig. 5D). However, these terminal arbors were unusually short (r=0.59, P=0.0000403, Fig. 5E). Although cluster 1 neurons are morphologically simple, all but one had at least one branch point (Fig. 5F). Cluster 1 neurons innervated all regions of the lingual epithelium (Fig. 5A, red arrowheads) including eight neurons innervated taste buds located at the tongue tip, twelve spanned between the tip and the mid-region, eleven innervated the tongue mid-region only, two innervated the back of the tongue, and three spanned between the mid-region and the back of the tongue.

Complex taste axons innervate additional taste buds.

Reconstructions of cluster 2 neurons illustrate an axon innervating three taste buds (Fig. 6A) and a second axon innervating seven taste buds (Fig. 6B). The neuron illustrated in Fig. 6A has widened endings (blue arrows), which were present in most taste nerve terminal arbors; a feature that did not differ across clusters. Although the function of these endings is not known, flattened contacts with receptor cells or retraction bulbs are possibilities (Bernstein and Lichtman 1999, Zaidi, Cicchini et al. 2016). Compared to those in cluster 1, axons of cluster 2 neurons contained more branch points in the tongue muscle and lamina propria (median=1 (N=42) vs 4 (N=36), U=254, P<0.001) and innervated more taste buds (Fig. 6C, median=2 (N=42) vs 3 (N=36), U=296, P<0.001); Thus, the entire axon innervating the tongue was longer on average for cluster 2 axons than for cluster 1 axons (q=6.67,p=0.001, Fig. 6D). Similar to cluster 1, most of the axons of cluster 2 neurons had a single terminal arbor innervating each taste bud (Fig. 6A and B). Cluster 1 and cluster 2 neurons did not differ in the mean branch ends per arbor (median=2 (N=42) vs 2 (N=36), U=742, P=0.89) or mean terminal arbor length (median=20.8 (N=42) vs 24.6 (N=36) µm, U=575, P=0.07). Therefore, the longer combined terminal arbor length of cluster 2 axons reflects the larger number of taste buds innervated (Fig. 6E). There were cluster 2 neurons that innervated only 1 or 2 taste buds; however, these neurons had longer terminal arbors. This is represented by the significant inverse relationship between the number of taste buds innervated and the average terminal length of the arbors per taste bud (*r*=-0.81, p=0.00000000320, Fig. 6F). Like cluster 1, the axons of cluster 2 neurons innervated all regions of the lingual epithelium, but they were more likely to innervate multiple tongue regions.

The most complex peripheral taste axons innervate taste buds with multiple terminal arbors.

Representative examples of cluster 3 (Fig. 7A) and cluster 4 (Fig. 7B) neurons illustrate their greater complexity. Cluster 3/4 neurons innervate a similar number of taste buds as those in cluster 2 (Fig. 6C, mean=3.53 (N=36) vs 4.22 (N=18), t=-1.445, P=0.154), but with significantly more terminal arbors (Fig. 7C, median=5 (N=36) vs 8 (N=18), U=108, P<0.001). For example, seven taste buds were innervated by either 9 (Fig. 7A) or 10 (Fig. 7B) terminal arbors. Similar to these examples the number of arbors per taste bud was significantly higher than for cluster 1 and 2 neurons (Fig. 7D, median=1.33 (N=36) vs 1.83 (N=18), U=173, P=0.006). Since the mean length of each arbor did not differ among the clusters (H (2,93)=7.18, *P*=0.066), the increase in combined length of the terminal arbor inside the taste bud was attributable to the greater total number of arbors across clusters (r=0.74, p=3.44 X 10^{-18}, Fig. 7E). The only difference between neurons in clusters 3 and 4 is the combined lengths of the terminal arbors (Fig. 4C).

All clusters had axons with branches ending outside of taste buds (Fig. 7A and F). Neurons with these “non-taste” endings typically have one or more branches that penetrate the epithelium, with a free nerve ending in a region of the tongue not occupied by a taste bud. In some cases, these are entirely different arbors, but they could also be on an arbor that also innervates the taste bud. For example, the arbor of the first taste bud shown in Fig. 7A (dark blue) has a single branch arising from a branch point at the taste bud base (blue arrow) extending into the lingual epithelium. A total of 18 neurons had these non-taste endings, which were most often in fungiform papillae (13 neurons) but also in filiform papillae (3 neurons) or both (2 neurons).

Each terminal arbor contacts a limited number of receptor cells.

Clusters were best separated by the combined terminal arbor length in taste buds, which is the amount of axon available to contact receptor cells. Next, we sought to examine how many taste receptor cells are contacted by a single neuron. Communication from receptor cells to nerve arbors occur through both conventional synapses (Murray 1986, Kinnamon, Sherman et al. 1988, Yee, Yang et al. 2001) and release of ATP through CALHM1/3 channels (Taruno, Vingtdeux et

al. 2013, Ma, Taruno et al. 2018, Romanov, Lasher et al. 2018). Unfortunately, it is not possible to observe these connections with light microscopy. However, an axonal arbor and receptor cell must come sufficiently close that they cannot be distinguished as separate objects at the resolution of the light microscope (within 200nm) for these connections to occur (Corson and Erisir 2013). Therefore, the largest number of taste receptor cells that are sufficiently close to a neuron to form a connection can be determined. To determine the closest proximity between receptor cells and nerve fibers, we labeled all taste nerve arbors (Phox2b-Cre:tdTomato mice) and many taste receptor cells using well-established markers for cells transducing sweet, bitter, and umami-type stimuli [(anti-phospholipase C beta-2 (PLCβ2) (Zhao, Zhang et al. 2003, Clapp, Yang et al. 2004)] and those transducing sour-stimuli [(anti-carbonic anhydrase 4 (Car4) (Chandrashekar, Yarmolinsky et al. 2009)]. We then analyzed three-dimensional (3D) image stacks to identify the taste receptor cells and nerve arbors that were closest to each other using a computer algorithm that measures proximity (Fig. 7A,). We found that nerve arbors tended to be either within one voxel (~110nm, below the resolution of the light microscope and frequently seen as overlapping (referred to henceforth as contacts) or separated by more than 1µm (Fig. 6B). The micron separation between non-overlapping nerve fibers and receptor cells is likely due to the unlabeled supporting cells that comprise the bulk of the taste bud (Yang, Dzowo et al. 2019), which have processes that wrap around nerve arbors and receptor cells (Bartel, Sullivan et al. 2006). While individual contacts may not be particularly meaningful, numbers or patterns can be compared across groups. For example, taste neurons expressing the serotonin receptor contact more sour receptor cells (which produce serotonin) than other cell types (Stratford, Larson et al. 2017).

To determine how many receptor cells are contacted by individual taste arbors, we traced 151 individual arbors in fungiform taste buds. For arbors contacting either PLCβ2-labeled receptor cells or Car4 receptor cells, some arbors followed the receptor cell a considerable distance (12-25µ; Fig. 8C, E), and others for much shorter distances (less than 12µm, Fig. 8D,F). Frequently,

arbors contact the same cell at multiple different locations. Because it is unclear how many of these contacts actually represent a connection, we did not quantify contacts, but the number of cells contacted. Thus, an arbor contacts one cell regardless of the distance travelled along the cell or the number of distinct instances with which the two cells come within 200nm. Using this analysis, we found that each arbor contacted 1.87 receptor cells on average. This number is only slightly more than the average of 1.6 receptor cells that synapse with individual circumvallate arbors (Kinnamon, Sherman et al. 1988).

We found that 47% of the arbors only contacted one receptor cell, suggesting that these arbors form a connection with a single taste receptor cell or lacked a connection altogether. A few of the arbors contacted no receptor cells (7%) and could not receive input from either a Car4-positive or PLCβ2-positive receptor cell. Of those that contacted multiple cells, 26 contacted cells of the same type (17%; only Car4- or only PLCβ2-positive cells) and 43 contacted both types (28%; PLCβ2- and Car4-labeled receptor cells). In addition to functional connections, an arbor likely contacts a receptor cell when assessing molecular compatibility (Lee, Macpherson et al. 2017) to form a new connection and on accident. Because there is no evidence that an individual arbor can received function input from more than one receptor cell type, we speculated that arbors contacting more than one cell type might be larger, and perhaps in a state of greater plasticity (process of connecting to a new cell). Consistent with this possibility, arbors contacting more than one cell type are longer (median=89 (N=106) vs 57 (N=39) µm, U=1185, P=0.0001) and more heavily branched (median 5 (N=106) vs 3 branch ends (N=39), U=1522, P=0.0012).

Complex neurons contact more receptor cells than simply branched neurons.

Next, we sought to examine the possibility that more heavily branched neurons have an opportunity to connect with more receptor cells. To this end, we labeled only one axon entering each half of the tongue, so that all the individual arbors identified were from the same neuron. Since these neurons typically do not cross the midline, each half of the tongue can be evaluated

independently. Individual axons were identified from where the chorda tympani-lingual nerve enters the tongue in a single nerve bundle and followed through multiple serial sections to determine the number of labeled axons (Fig. 9A). By injecting different low doses of tamoxifen (0.3–0.6 mg), we determined that one injection of 0.6 mg results in one single labeled axon roughly 25% of the time. For each axon verified as a single labeled axon in one tongue half, all 40–45 taste buds on that side of the tongue were immunolabeled and scanned by confocal microscopy to identify and reconstruct each terminal arbor. Two examples of cluster 1 neurons are illustrated (Figure 9B,). The first neuron innervated one taste bud and contacted two Car4-positive cells. The second neuron innervated two taste buds and contacted 4 PLCβ2-positive cells. A single cluster 2 neuron is also illustrated (Fig. 9C), which contacted 10 receptor cells across 5 taste buds. Although this axon contacts multiple receptor cell types, the contacts were heavily biased toward Car4-positive cells (7 Car4 and 3 PLCβ2).

A total of 21 single axons from clusters 1, 2, and 3 were analyzed. We found that the mean number of receptor cells contacted significantly differed between clusters ($H_{(2,20)}$=17.16 *P*=0.0002;Kruskal-Wallis; Fig. 9D). In fact, most cluster 1 neurons only contact one receptor cell. This finding indicates that either many taste neurons are either unresponsive to stimuli or a neuron response can be driven by input from only a single receptor cell. Therefore, a specific feature of cluster 1 neurons is that each of their arbors contacts fewer taste receptor cells (0.93 receptor cells/arbor) than is typical for the full population (1.8 receptor cells/arbor) ($U_{(1,48)}$=49, *P*=0.0006,Mann-Whitney), even though the arbors of these neurons were the same length ($H_{(2,76)}$=3.5, *P*=0.17, Kruskal-Wallis) and had the same number of branch ends ($H_{(2,76)}$=2.37, *P*=.31) across clusters. Thus, by increasing neuron complexity, taste neurons increase the number of receptor cells from which they could receive input.

Another difference across these morphological clusters was the pattern in the type of receptor cells contacted across the clusters (Fig. 9E). Arbors from the cluster 1 neurons are more likely to contact a PLCβ2 cell and less likely to Car4 cells than clusters 2 and 3 (χ^2 =6.63, p=0.036).

We examined this same question another way using a similar approach as functional studies. Functionally, gustatory neurons are typically divided based on their “best” stimulus quality (sweet, sour, etc.), even though roughly 40% of the population responds to more than one stimulus (Frank 2000, Yoshida, Yasumatsu et al. 2006, Barretto, Gillis-Smith et al. 2015, Wu, Dvoryanchikov et al. 2015). We speculated that a similar approach would permit us to compare morphologies across predicted functional quality by dividing neurons based on the type of cell contacted most frequently, PLCβ2 (sweet/bitter) or Car4 (sour) cells. For example, the neuron in Figure 9C contacted 7 Car4-positive cells and 3 PLCβ2-positive cells, so it was placed in the group contacting more Car4 cells. The two neurons that contact the same number of each cell type were placed into groups based on the size of these contacts. Of the 21 neurons examined, 11 contacted more sweet/bitter/umami cells, while 10 contacted more sour-transducing cells. Neurons contacting more sour-transducing cells had a greater combined terminal arbor length ($t=2.28$, $p=0.03$) indicating that they are more heavily branched than neurons primarily contacting sweet/bitter/umami-transducing cells. However, there was also considerable variation with in each group and distributions were overlapping.

Authors declare no competing interests

Discussion

Taste neurons exhibit both functional (Frank 1973, Lundy and Contreras 1999, Frank 2000, Sollars and Hill 2005, Yoshida, Yasumatsu et al. 2006, Breza, Nikonov et al. 2010, Yoshida and Ninomiya 2010, Barretto, Gillis-Smith et al. 2015, Wu, Dvoryanchikov et al. 2015) and genetic diversity (Yee, Yang et al. 2001, Zhang, Jin et al. 2019). Our goal was to determine if they are also morphologically diverse. Using sparse-cell genetic labeling, we found considerable variation in the branching characteristics of taste neurons. Roughly half of the taste neurons had few branches (cluster 1), whereas others branched extensively along a continuum of complexity. Axons of cluster 2 neurons had more arbors and innervated more taste buds than cluster 1 neurons (maximum 7 taste buds). Whereas axons of cluster 3 and 4 neurons innervated a similar number of taste buds as cluster 2 neurons, but had more terminal arbors per taste bud (maximum 17 arbors). This variability in branching complexity likely introduces variation in the amount of convergence of taste receptor cell input onto individual neurons. We were able to determine the largest possible number of potential connections for 21 neurons. We found that simple neurons (cluster 1) typically only contacted 1–4 taste receptor cells, whereas more heavily branched cluster 2 and 3 neurons could potentially receive input from 5–22 receptor cells. In addition, more heavily branched neurons were more likely to contact sour-transducing cells than those that transduce sweet/better/umami, indicating that neuron types likely differ in morphology. Lastly, variation in morphology within a neuron type or quality is also likely and has important implications for both function and plasticity.

To what extent the variable morphological complexities represent a snap-shot in time of a changing pattern or are permanent characteristics is unclear. A unique feature of taste receptor cells is that they have a limited lifespan and are constantly renewed (Beidler and Smallman 1965, Farbman 1980, Delay, Kinnamon et al. 1986, Perea-Martinez, Nagai et al. 2013). As a result, gustatory ganglion neurons must continually locate and form functional connections with new adult taste receptor cells. Presumably, this process is accompanied by changes in branching

characteristics. We observed substantial variation in neuron complexity which predicts differences in the number of receptor cells contacted by individual neurons. If branching changes over time, degree of convergence could also be a changing feature of taste neurons resulting in changing functional characteristics over time (Shimatani, Nikles et al. 2003). However, this may be true only within a limited range, if some components of the neuron structure are stable over time.

One possibility is that arbor complexity is dictated primarily by the process of finding and connecting with a new receptor cell, while arbor number is a stable feature of the neuron. We found no differences in mean arbor length or complexity across clusters, consistent with the idea that arbor structure is primarily plastic. The largest/most complex arbors could be extending throughout the taste bud to locate and connect to a new receptor cell. Consistently, arbors contacting multiple cell types were longer and more heavily branched. In spite of their variable morphology, most terminal arbors only contact 1-2 receptor cells, which is consistent with electron microscopy findings for synapses (Kinnamon, Sherman et al. 1988). Consistently, we found that the number of terminal arbors is the best predictor of the number of receptor cells contacted by an individual neuron. The number of terminal arbors is determined by the number of branch points outside the taste bud. Because a change in these branch points may not be required for a taste bud to form a new connection with a receptor cell, the number of arbors may be a stable characteristic of the neuron. Because number of arbors determines the number of receptor cells contacted this could contribute to functional stability over time.

We examined the number of receptor cells contacted by each neuron. Contacts likely represent one of three scenarios, only one of which represents functional connectivity. First, there are likely some locations where the nerve arbor simply passes within 200nm of a receptor cell without any specific interaction with that cell. A second possibility are locations where the cell membranes of neurons and receptor cells contact as part of the process of re-innervation with cell turnover (as discussed above). Contact between receptor cells and nerve arbors would allow a nerve arbor to determine molecular compatibility (i.e. the presence of a ligand on one cell and

receptor on the other for factors involved in synapse formation). These “sampling contacts” are likely since the continued rewiring of the taste system is thought to depend upon multiple molecular factors (Lee, Macpherson et al. 2017). The third scenario is that all functional connections require a contact measurable at the light level. Distinguishing between these possibilities for an individual neuron is not possible even with EM analysis (Yang, Dzowo et al. 2019). This is the case because individual arbors from the same neuron are separated by too great a distance to be reconstructed at the EM level. In addition, structural corelates do not exist between nerve fibers and all cell types, in spite of recent advances (Romanov, Lasher et al. 2018). However, it seems likely that the number of functional connections is greater in neurons with many arbors than for neurons with only a single arbor. If each neuron only had a functional connection on only one arbor, regardless the number arbors, only 96 of the 452 arbors we observed would have a connection, leaving 78% of all arbors without a connection to a taste receptor cell – a possibility which is not consistent with EM studies (Kinnamon, Sherman et al. 1988). Thus, the most likely reason for differential branching is differential convergence.

Variations in the amount of convergent input from the same type of receptor onto different neurons could result in variable sensitivities to the taste stimulus transduced by these cells. For example, a neuron receiving input from eight sour-transducing receptor cells (Car4 expressing (Huang, Chen et al. 2006, Chandrashekar, Yarmolinsky et al. 2009)) may be more sensitive to citric acid than a neuron receiving input from only two sour transducing receptor cells. Consistent with this idea, stimulation of independent areas of a neuron’s receptive field with the same stimulus enhances the response (Miller 1971). Our results show that not all neurons branch to contact multiple receptor cells, suggesting that this enhancement occurs in some neurons, but not others. These differences could produce variations in thresholds and intensity ranges for the same stimulus across the population of neurons. While increases in response rate represent taste stimulus intensity (Ganchrow and Erickson 1970, Scott, Plata-Salaman et al. 1991, Breza, Nikonov et al. 2010, Fonseca, de Lafuente et al. 2018), it is unclear whether additional peripheral

neurons are recruited as stimulus intensity increases (i.e. graded intensity coding), as is the case with warm stimuli (Wang, Belanger et al. 2018). Variation in stimulus thresholds across the population is consistent with our anatomical data and would permit a greater range of intensities to be coded by taste neurons than by individual taste receptor cells (Caicedo, Kim et al. 2002). This possibility is supported by the findings from the few studies that utilized multiple stimulus concentrations to examine taste coding in peripheral neurons (Ganchrow and Erickson 1970, Breza, Nikonov et al. 2010, Wu, Dvoryanchikov et al. 2015). Consistent with this idea, our data predict a range of branching characteristics within each taste quality.

We also observed that neurons contacting more sour-transducing receptor cells tended to be more heavily branched than those contacting sweet/bitter/umami transducing receptor cells. If as a result, neurons responding to sour stimuli receive input from a larger number of taste receptor cells, they would be predicted to be more broadly tuned. Approximately one-fourth of individual taste receptor cells are capable of responding to more than one stimulus (Tomchik, Berg et al. 2007, Yoshida and Ninomiya 2016). Therefore, as the amount of convergent input increases for a given neuron, the probability that it will receive input from receptor cells responding to multiple stimuli also increases. Variation in branching may explain why functional studies of peripheral taste neurons have consistently observed both narrowly and broadly tuned neurons (Yoshida, Yasumatsu et al. 2006, Barretto, Gillis-Smith et al. 2015, Wu, Dvoryanchikov et al. 2015). Consistently, neurons responding to sweet are typically described as more narrowly tuned than neurons responding to primarily to sour (Lundy and Contreras 1999, Frank 2000, Breza, Nikonov et al. 2010). While it has been repeatedly speculated that this is due to differences in the tuning properties of the taste receptor cells (Tomchik, Berg et al. 2007, Barretto, Gillis-Smith et al. 2015), our data suggest that differential convergence onto the nerve fiber is another likely explanation.

Authors declare no competing interests

References

Abraira, V. E. and D. D. Ginty (2013). "The sensory neurons of touch." Neuron **79**(4): 618-639.

Bachmanov, A. A., M. G. Tordoff and G. K. Beauchamp (1996). "Ethanol consumption and taste preferences in C57BL/6ByJ and 129/J mice." Alcohol Clin Exp Res **20**(2): 201-206.

Badea, T. C., Y. Wang and J. Nathans (2003). "A noninvasive genetic/pharmacologic strategy for visualizing cell morphology and clonal relationships in the mouse." J Neurosci **23**(6): 2314-2322.

Badea, T. C., J. Williams, P. Smallwood, M. Shi, O. Motajo and J. Nathans (2012). "Combinatorial expression of Brn3 transcription factors in somatosensory neurons: genetic and morphologic analysis." J Neurosci **32**(3): 995-1007.

Bai, L., B. P. Lehnert, J. Liu, N. L. Neubarth, T. L. Dickendesher, P. H. Nwe, C. Cassidy, C. J. Woodbury and D. D. Ginty (2015). "Genetic Identification of an Expansive Mechanoreceptor Sensitive to Skin Stroking." Cell **163**(7): 1783-1795.

Barretto, R. P., S. Gillis-Smith, J. Chandrashekar, D. A. Yarmolinsky, M. J. Schnitzer, N. J. Ryba and C. S. Zuker (2015). "The neural representation of taste quality at the periphery." Nature **517**(7534): 373-376.

Bartel, D. L., S. L. Sullivan, E. G. Lavoie, J. Sevigny and T. E. Finger (2006). "Nucleoside triphosphate diphosphohydrolase-2 is the ecto-ATPase of type I cells in taste buds." J Comp Neurol **497**(1): 1-12.

Beidler, L. M. and R. L. Smallman (1965). "Renewal of cells within taste buds." J Cell Biol **27**(2): 263-272.

Bernstein, M. and J. W. Lichtman (1999). "Axonal atrophy: the retraction reaction." Curr Opin Neurobiol **9**(3): 364-370.

Breza, J. M., K. S. Curtis and R. J. Contreras (2006). "Temperature modulates taste responsiveness and stimulates gustatory neurons in the rat geniculate ganglion." J Neurophysiol **95**(2): 674-685.

Breza, J. M., A. A. Nikonov and R. J. Contreras (2010). "Response latency to lingual taste stimulation distinguishes neuron types within the geniculate ganglion." J Neurophysiol **103**(4): 1771-1784.

Caicedo, A., K. N. Kim and S. D. Roper (2002). "Individual mouse taste cells respond to multiple chemical stimuli." J Physiol **544**(2): 501-509.

Carleton, A., R. Accolla and S. A. Simon (2010). "Coding in the mammalian gustatory system." Trends Neurosci **33**(7): 326-334.

Castillo, K., I. Diaz-Franulic, J. Canan, F. Gonzalez-Nilo and R. Latorre (2018). "Thermally activated TRP channels: molecular sensors for temperature detection." Phys Biol **15**(2): 021001.

Chandrashekar, J., M. A. Hoon, N. J. Ryba and C. S. Zuker (2006). "The receptors and cells for mammalian taste." Nature **444**(7117): 288-294.

Chandrashekar, J., D. Yarmolinsky, L. von Buchholtz, Y. Oka, W. Sly, N. J. Ryba and C. S. Zuker (2009). "The taste of carbonation." Science **326**(5951): 443-445.

Chklovskii, D. B. (2004). "Synaptic connectivity and neuronal morphology: two sides of the same coin." Neuron **43**(5): 609-617.

Clapp, T. R., R. Yang, C. L. Stoick, S. C. Kinnamon and J. C. Kinnamon (2004). "Morphologic characterization of rat taste receptor cells that express components of the phospholipase C signaling pathway." J Comp Neurol **468**(3): 311-321.

Contreras, R. J. and R. F. Lundy (2000). "Gustatory neuron types in the periphery: a functional perspective." Physiol Behav **69**(1-2): 41-52.

Corson, J. A. and A. Erisir (2013). "Monosynaptic convergence of chorda tympani and glossopharyngeal afferents onto ascending relay neurons in the nucleus of the solitary

tract: a high-resolution confocal and correlative electron microscopy approach." J Comp Neurol **521**(13): 2907-2926.
Delay, R. J., J. C. Kinnamon and S. D. Roper (1986). "Ultrastructure of mouse vallate taste buds: II. Cell types and cell lineage." J Comp Neurol **253**(2): 242-252.
Dvoryanchikov, G., D. Hernandez, J. K. Roebber, D. L. Hill, S. D. Roper and N. Chaudhari (2017). "Transcriptomes and neurotransmitter profiles of classes of gustatory and somatosensory neurons in the geniculate ganglion." Nat Commun **8**(1): 760.
Farbman, A. I. (1980). "Renewal of taste bud cells in rat circumvallate papillae." Cell Tissue Kinet **13**(4): 349-357.
Fonseca, E., V. de Lafuente, S. A. Simon and R. Gutierrez (2018). "Sucrose intensity coding and decision-making in rat gustatory cortices." Elife **7**.
Frank, M. (1973). "An analysis of hamster afferent taste nerve response functions." J Gen Physiol **61**(5): 588-618.
Frank, M. E. (2000). "Neuron types, receptors, behavior, and taste quality." Physiol Behav **69**(1-2): 53-62.
Ganchrow, J. R. and R. P. Erickson (1970). "Neural correlates of gustatory intensity and quality." J Neurophysiol **33**(6): 768-783.
Guagliardo, N. A. and D. L. Hill (2007). "Fungiform taste bud degeneration in C57BL/6J mice following chorda-lingual nerve transection." J Comp Neurol **504**(2): 206-216.
Huang, A. L., X. Chen, M. A. Hoon, J. Chandrashekar, W. Guo, D. Trankner, N. J. Ryba and C. S. Zuker (2006). "The cells and logic for mammalian sour taste detection." Nature **442**(7105): 934-938.
Huang, T. and R. F. Krimm (2010). "Developmental expression of Bdnf, Ntf4/5, and TrkB in the mouse peripheral taste system." Dev Dyn **239**(10): 2637-2646.
Kinnamon, J. C., T. A. Sherman and S. D. Roper (1988). "Ultrastructure of mouse vallate taste buds: III. Patterns of synaptic connectivity." J Comp Neurol **270**(1): 1-10, 56-17.
Kuehn, E. D., S. Meltzer, V. E. Abraira, C. Y. Ho and D. D. Ginty (2019). "Tiling and somatotopic alignment of mammalian low-threshold mechanoreceptors." Proc Natl Acad Sci U S A **116**(19): 9168-9177.
Lee, H., L. J. Macpherson, C. A. Parada, C. S. Zuker and N. J. P. Ryba (2017). "Rewiring the taste system." Nature **548**(7667): 330-333.
Liebl, D. J., J. P. Mbiene and L. F. Parada (1999). "NT4/5 mutant mice have deficiency in gustatory papillae and taste bud formation." Dev Biol **213**(2): 378-389.
Lim, J. and A. J. Pullicin (2019). "Oral carbohydrate sensing: Beyond sweet taste." Physiol Behav **202**: 14-25.
Liu, D., N. Archer, K. Duesing, G. Hannan and R. Keast (2016). "Mechanism of fat taste perception: Association with diet and obesity." Prog Lipid Res **63**: 41-49.
Lundy, R. F., Jr. and R. J. Contreras (1997). "Temperature and amiloride alter taste nerve responses to Na+, K+, and NH+4 salts in rats." Brain Res **744**(2): 309-317.
Lundy, R. F., Jr. and R. J. Contreras (1999). "Gustatory neuron types in rat geniculate ganglion." J Neurophysiol **82**(6): 2970-2988.
Ma, Z., A. Taruno, M. Ohmoto, M. Jyotaki, J. C. Lim, H. Miyazaki, N. Niisato, Y. Marunaka, R. J. Lee, H. Hoff, R. Payne, A. Demuro, I. Parker, C. H. Mitchell, J. Henao-Mejia, J. E. Tanis, I. Matsumoto, M. G. Tordoff and J. K. Foskett (2018). "CALHM3 Is Essential for Rapid Ion Channel-Mediated Purinergic Neurotransmission of GPCR-Mediated Tastes." Neuron **98**(3): 547-561 e510.
Maksimovic, S., M. Nakatani, Y. Baba, A. M. Nelson, K. L. Marshall, S. A. Wellnitz, P. Firozi, S. H. Woo, S. Ranade, A. Patapoutian and E. A. Lumpkin (2014). "Epidermal Merkel cells are mechanosensory cells that tune mammalian touch receptors." Nature **509**(7502): 617-621.

Authors declare no competing interests

Miller, I. J., Jr. (1971). "Peripheral interactions among single papilla inputs to gustatory nerve fibers." J Gen Physiol **57**(1): 1-25.
Murray, R. G. (1986). "The mammalian taste bud type III cell: a critical analysis." J Ultrastruct Mol Struct Res **95**(1-3): 175-188.
Ohla, K., R. Yoshida, S. D. Roper, P. M. Di Lorenzo, J. D. Victor, J. D. Boughter, M. Fletcher, D. B. Katz and N. Chaudhari (2019). "Recognizing taste: coding patterns along the neural axis in mammals." Chem Senses.
Ohman-Gault, L., T. Huang and R. Krimm (2017). "The transcription factor Phox2b distinguishes between oral and non-oral sensory neurons in the geniculate ganglion." J Comp Neurol **525**(18): 3935-3950.
Patel, A. V. and R. F. Krimm (2012). "Neurotrophin-4 regulates the survival of gustatory neurons earlier in development using a different mechanism than brain-derived neurotrophic factor." Dev Biol **365**(1): 50-60.
Perea-Martinez, I., T. Nagai and N. Chaudhari (2013). "Functional cell types in taste buds have distinct longevities." PLoS One **8**(1): e53399.
Rios-Pilier, J. and R. F. Krimm (2019). "TrkB expression and dependence divides gustatory neurons into three subpopulations." Neural Dev **14**(1): 3.
Romanov, R. A., R. S. Lasher, B. High, L. E. Savidge, A. Lawson, O. A. Rogachevskaja, H. Zhao, V. V. Rogachevsky, M. F. Bystrova, G. D. Churbanov, I. Adameyko, T. Harkany, R. Yang, G. J. Kidd, P. Marambaud, J. C. Kinnamon, S. S. Kolesnikov and T. E. Finger (2018). "Chemical synapses without synaptic vesicles: Purinergic neurotransmission through a CALHM1 channel-mitochondrial signaling complex." Sci Signal **11**(529).
Rutlin, M., C. Y. Ho, V. E. Abraira, C. Cassidy, C. J. Woodbury and D. D. Ginty (2014). "The cellular and molecular basis of direction selectivity of Adelta-LTMRs." Cell **159**(7): 1640-1651.
Scott, T. R., C. R. Plata-Salaman, V. L. Smith and B. K. Giza (1991). "Gustatory neural coding in the monkey cortex: stimulus intensity." J Neurophysiol **65**(1): 76-86.
Shimatani, Y., S. A. Nikles, K. Najafi and R. M. Bradley (2003). "Long-term recordings from afferent taste fibers." Physiol Behav **80**(2-3): 309-315.
Sollars, S. I. and D. L. Hill (2005). "In vivo recordings from rat geniculate ganglia: taste response properties of individual greater superficial petrosal and chorda tympani neurones." J Physiol **564**(Pt 3): 877-893.
Spector, A. C. and S. P. Travers (2005). "The representation of taste quality in the mammalian nervous system." Behav Cogn Neurosci Rev **4**(3): 143-191.
Stratford, J. M., E. D. Larson, R. Yang, E. Salcedo and T. E. Finger (2017). "5-HT3A -driven green fluorescent protein delineates gustatory fibers innervating sour-responsive taste cells: A labeled line for sour taste?" J Comp Neurol **525**(10): 2358-2375.
Sun, C., A. Dayal and D. L. Hill (2015). "Expanded terminal fields of gustatory nerves accompany embryonic BDNF overexpression in mouse oral epithelia." J Neurosci **35**(1): 409-421.
Tang, T., J. Rios-Pilier and R. Krimm (2017). "Taste bud-derived BDNF maintains innervation of a subset of TrkB-expressing gustatory nerve fibers." Mol Cell Neurosci **82**: 195-203.
Taruno, A., V. Vingtdeux, M. Ohmoto, Z. Ma, G. Dvoryanchikov, A. Li, L. Adrien, H. Zhao, S. Leung, M. Abernethy, J. Koppel, P. Davies, M. M. Civan, N. Chaudhari, I. Matsumoto, G. Hellekant, M. G. Tordoff, P. Marambaud and J. K. Foskett (2013). "CALHM1 ion channel mediates purinergic neurotransmission of sweet, bitter and umami tastes." Nature **495**(7440): 223-226.
Tomchik, S. M., S. Berg, J. W. Kim, N. Chaudhari and S. D. Roper (2007). "Breadth of tuning and taste coding in mammalian taste buds." J Neurosci **27**(40): 10840-10848.
Tordoff, M. G. (2001). "Calcium: taste, intake, and appetite." Physiol Rev **81**(4): 1567-1597.
Tordoff, M. G. (2017). "Phosphorus Taste Involves T1R2 and T1R3." Chem Senses **42**(5): 425-433.

Authors declare no competing interests

Valm, A. M., S. Cohen, W. R. Legant, J. Melunis, U. Hershberg, E. Wait, A. R. Cohen, M. W. Davidson, E. Betzig and J. Lippincott-Schwartz (2017). "Applying systems-level spectral imaging and analysis to reveal the organelle interactome." Nature **546**(7656): 162-167.

Wang, F., E. Belanger, S. L. Cote, P. Desrosiers, S. A. Prescott, D. C. Cote and Y. De Koninck (2018). "Sensory Afferents Use Different Coding Strategies for Heat and Cold." Cell Rep **23**(7): 2001-2013.

Wu, A., G. Dvoryanchikov, E. Pereira, N. Chaudhari and S. D. Roper (2015). "Breadth of tuning in taste afferent neurons varies with stimulus strength." Nat Commun **6**: 8171.

Wu, H., J. Williams and J. Nathans (2012). "Morphologic diversity of cutaneous sensory afferents revealed by genetically directed sparse labeling." Elife **1**: e00181.

Wu, P., D. Arris, M. Grayson, C. N. Hung and S. Ruparel (2018). "Characterization of sensory neuronal subtypes innervating mouse tongue." PLoS One **13**(11): e0207069.

Yang, R., Y. K. Dzowo, C. E. Wilson, R. L. Russell, G. J. Kidd, E. Salcedo, R. S. Lasher, J. C. Kinnamon and T. E. Finger (2019). "Three-dimensional reconstructions of mouse circumvallate taste buds using serial blockface scanning electron microscopy: I. Cell types and the apical region of the taste bud." J Comp Neurol.

Yarmolinsky, D. A., C. S. Zuker and N. J. Ryba (2009). "Common sense about taste: from mammals to insects." Cell **139**(2): 234-244.

Yee, C. L., R. Yang, B. Bottger, T. E. Finger and J. C. Kinnamon (2001). ""Type III" cells of rat taste buds: immunohistochemical and ultrastructural studies of neuron-specific enolase, protein gene product 9.5, and serotonin." J Comp Neurol **440**(1): 97-108.

Yokota, Y. and R. M. Bradley (2016). "Receptive field size, chemical and thermal responses, and fiber conduction velocity of rat chorda tympani geniculate ganglion neurons." J Neurophysiol **115**(6): 3062-3072.

Yokota, Y. and R. M. Bradley (2017). "Geniculate Ganglion Neurons are Multimodal and Variable in Receptive Field Characteristics." Neuroscience **367**: 147-158.

Yoshida, R. and Y. Ninomiya (2010). "New insights into the signal transmission from taste cells to gustatory nerve fibers." Int Rev Cell Mol Biol **279**: 101-134.

Yoshida, R. and Y. Ninomiya (2016). "Taste information derived from T1R-expressing taste cells in mice." Biochem J **473**(5): 525-536.

Yoshida, R., K. Yasumatsu, N. Shigemura and Y. Ninomiya (2006). "Coding channels for taste perception: information transmission from taste cells to gustatory nerve fibers." Arch Histol Cytol **69**(4): 233-242.

Zaidi, F. N., V. Cicchini, D. Kaufman, E. Ko, A. Ko, H. Van Tassel and M. C. Whitehead (2016). "Innervation of taste buds revealed with Brainbow-labeling in mouse." J Anat **229**(6): 778-790.

Zaidi, F. N., R. F. Krimm and M. C. Whitehead (2007). "Exuberant neuronal convergence onto reduced taste bud targets with preservation of neural specificity in mice overexpressing neurotrophin in the tongue epithelium." J Neurosci **27**(50): 13875-13881.

Zaidi, F. N. and M. C. Whitehead (2006). "Discrete innervation of murine taste buds by peripheral taste neurons." J Neurosci **26**(32): 8243-8253.

Zhang, J., H. Jin, W. Zhang, C. Ding, S. O'Keeffe, M. Ye and C. S. Zuker (2019). "Sour Sensing from the Tongue to the Brain." Cell **179**(2): 392-402 e315.

Zhao, G. Q., Y. Zhang, M. A. Hoon, J. Chandrashekar, I. Erlenbach, N. J. Ryba and C. S. Zuker (2003). "The receptors for mammalian sweet and umami taste." Cell **115**(3): 255-266.

Authors declare no competing interests

Figures

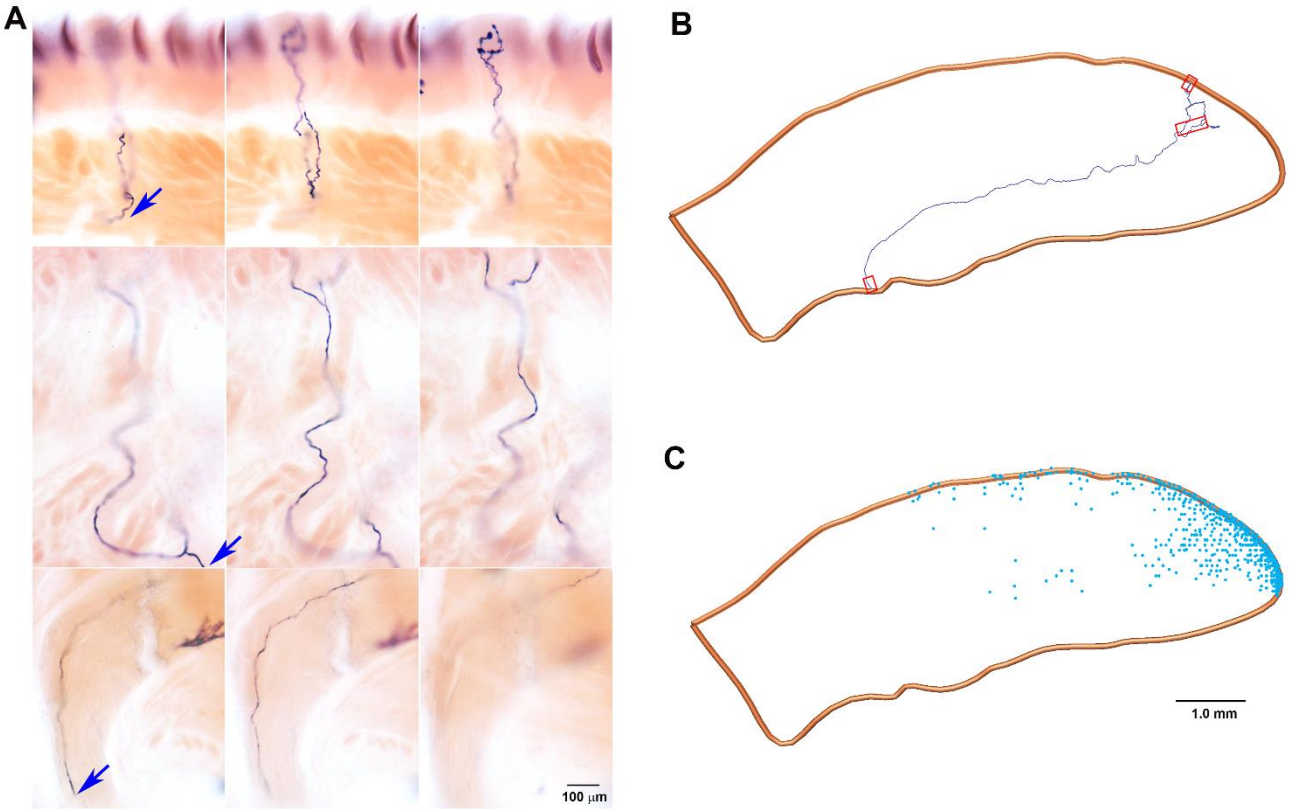

Figure 1. Genetically directed sparse-cell labeling and reconstruction of individual taste axons. (A) A single AP-stained axon from a *TrkB*^{CreER}:AP mouse injected with tamoxifen at postnatal day 40. The axon is shown at different locations within the tongue (top to bottom), indicated by the boxed areas in B. Each location is shown at 3 different focal depths (left to right) in this 180-µm section. Arrows indicate the ventral most point of the axons in each series of images. (B) A full reconstruction of the single taste axon in panel A from where it enters the tongue to the terminal arbors. It is superimposed on an outline of a tongue section. This axon innervates 2 taste buds (one of which is shown in A) and branches beneath the epithelium to penetrate the same taste bud with two simple terminal arbors (the portion of the axon that is within the taste bud). These arbors show prominent varicosities, which is a common feature of these axons once they have innervated the taste bud. (C) Locations of the branch points from 96 reconstructed axons in the tongue, illustrating that taste axons branch throughout the entire tongue. There were numerous branch points in the tongue muscle and lamina propria, most of which produced arbors that innervated separate taste buds. Branch points immediately below the taste bud result in a single neuron innervating the same taste bud with multiple separate terminal arbors. In addition, each terminal arbor entering a taste bud may branch considerably within the taste bud. The scale bar in A = 100µm; the scale bar for B and C = 1.0 mm.

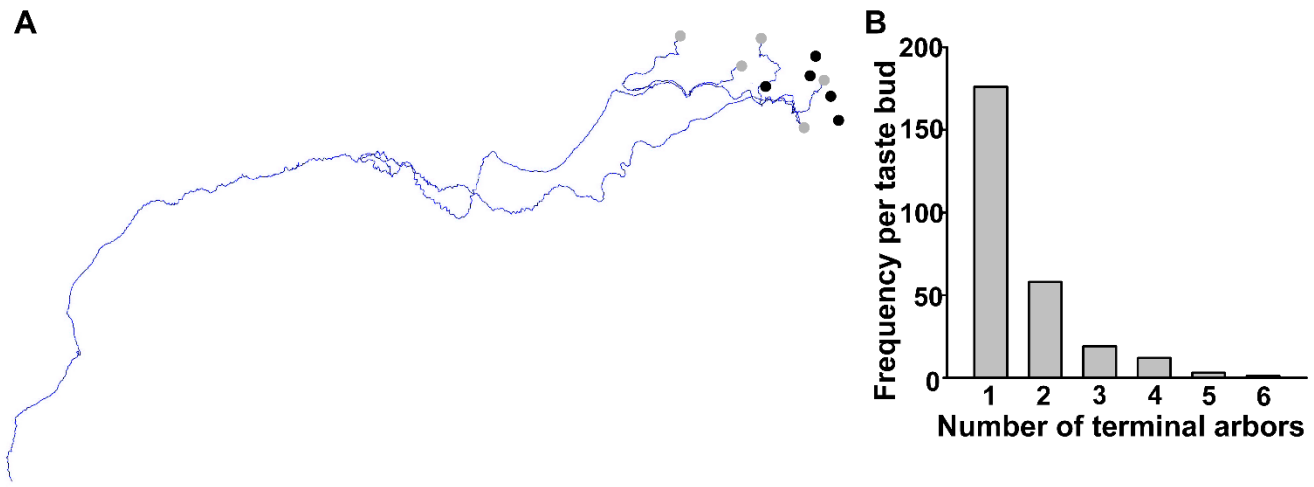

Figure 2. Individual neurons distribute arbors across anatomical receptive not always innervating adjacent papillae and innervating most taste buds with only a single arbor. (A) An example of an axon that innervated 5 taste buds. The fungiform papillae containing the innervated taste buds are marked by gray dots. Other fungiform papillae containing taste buds not innervated by this neuron (marked by black dots) and at least two are located between innervated papillae. (B) Histogram illustrating the number of taste buds innervated by 1 to 6 terminal arbors from the same neuron. Most taste buds only receive a single arbor from a single taste neuron.

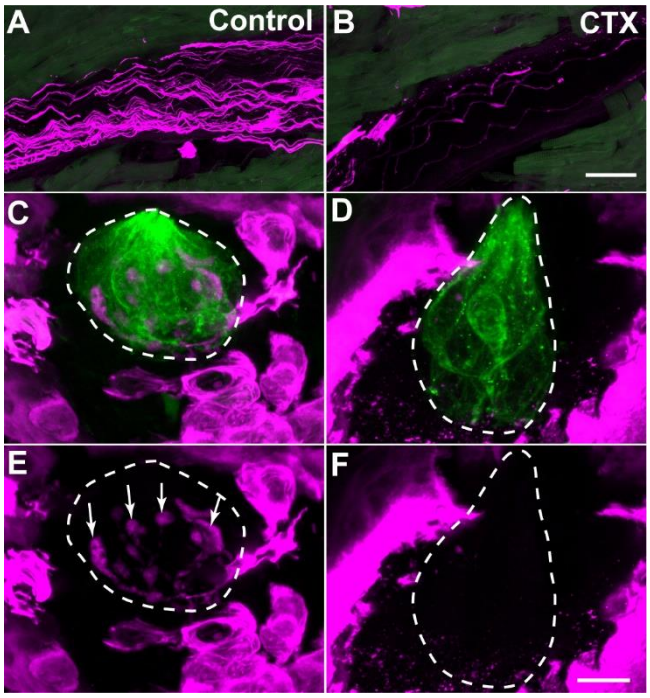

Figure 3. Chorda tympani nerve transection eliminates most TrkB-positive taste axons from the tongue and taste buds. (A-C) On the un-transected side of the tongue (intact), abundant TrkB-positive axons (magenta) were observed in chorda-lingual nerve bundles (B, C). In taste buds (outlined with white dots), TrkB-positive axons were clearly seen from the intact side of the tongue (indicated by arrows). With high doses of tamoxifen label is also present in most of the non-taste epithelia around the taste bud. (D-F) On the chorda tympani transected side of the tongue (CTX) from the same mouse, substantially fewer TrkB-positive axons were observed in nerve bundles. (E-F) On the CTX side of the tongue, taste buds lacked labeled axons. Scale bar in B =50µ and also applies to A; scale bar in F = 10µm and also applies to C, D, and E.

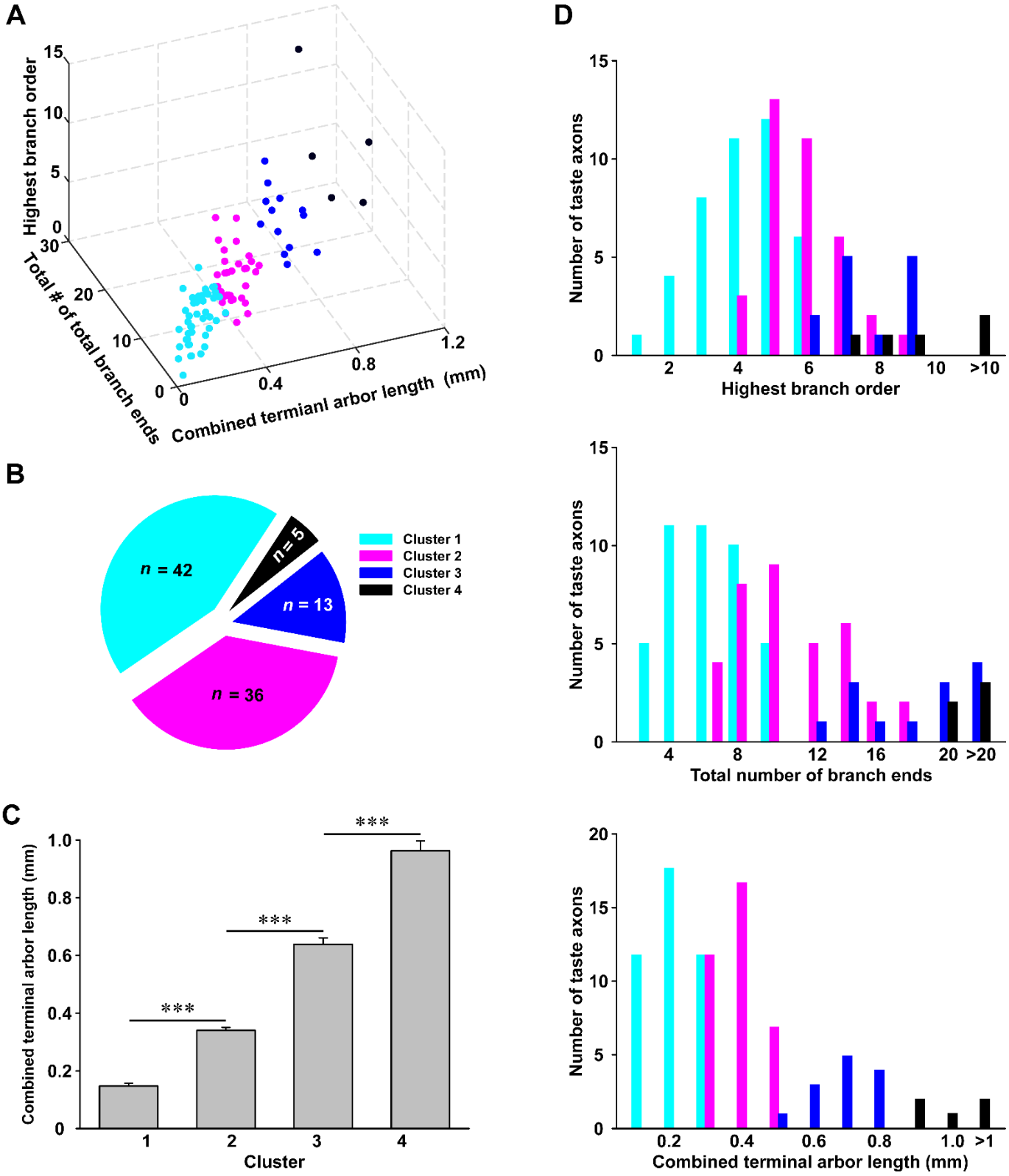

Figure 4. Taste axons were divided into four categories using a k-means cluster analysis. (A) 3D graph showing the three characteristics which best separate the axons into clusters. The axons demonstrate increasing branch complexity according to all three measures across the clusters. (B) The numbers of axons falling into each cluster are illustrated with a pie chart. (C) The combined terminal arbor length (across all arbors and taste buds) was the trait that most distinctly separated the axons into clusters and, therefore, is significantly different between the four clusters. (D) Frequency histograms of the three characteristics shown in A. ***$P \leq 0.001$

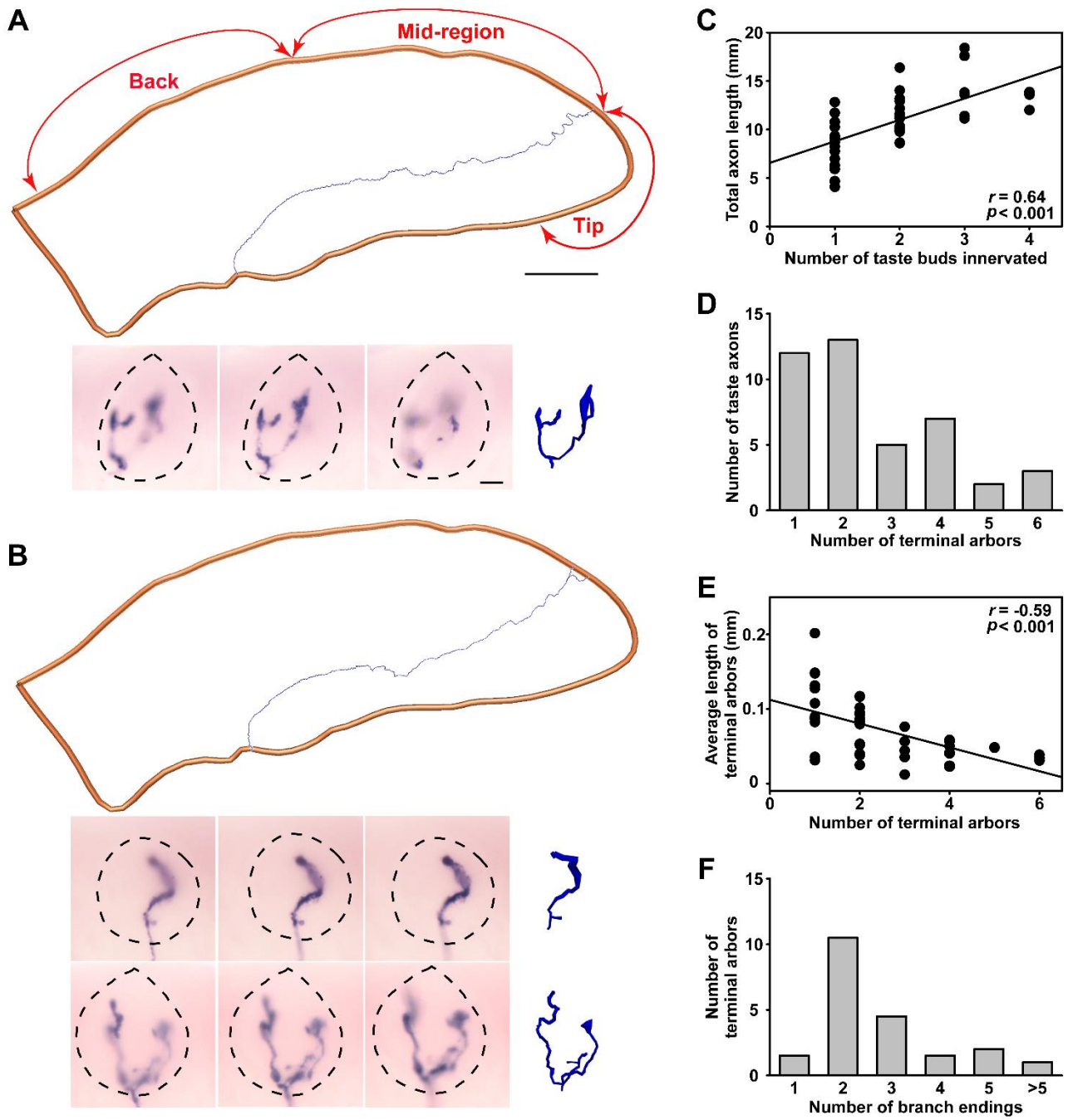

Figure 5. Two examples of the axons of cluster 1 neurons. (A, B) The reconstructed axons were superimposed on an outline of one sagittal tongue section to illustrate the location of the axon in the tongue. Red arrows in the panel divide the tongue into regions of the lingual epithelium: tip, mid-region, and back. The images below each reconstructed axon show the AP staining of a single terminal arbor within the taste bud at three different focal depths. Reconstructions of the terminal arbors within the taste bud are shown at the same magnification to the right of the images. (A) This 10.3-mm-long axon innervated a single taste bud with one terminal arbor, three branch points inside the taste bud, and four branch endings. (B) The second 14.0-mm-long axon innervated two taste buds with one terminal arbor each, one branch point outside the taste bud and four inside the taste bud, resulting in six terminal branch ends. (C) Cluster 1 taste axons innervate 1–4 taste buds; axons that branch to enter more taste buds have short terminal arbors. (D) The axons of cluster 1 neurons have as many as six separate terminal arbors penetrating taste buds. (E) The cluster 1 neurons with the most terminal arbors also had the shortest terminal arbors. (F) The distribution of the number of branch endings per terminal arbor. Scale bars: 1 mm for whole nerve tracings in A and B; 10 µm for taste bud images and reconstructions within taste buds in A and B.

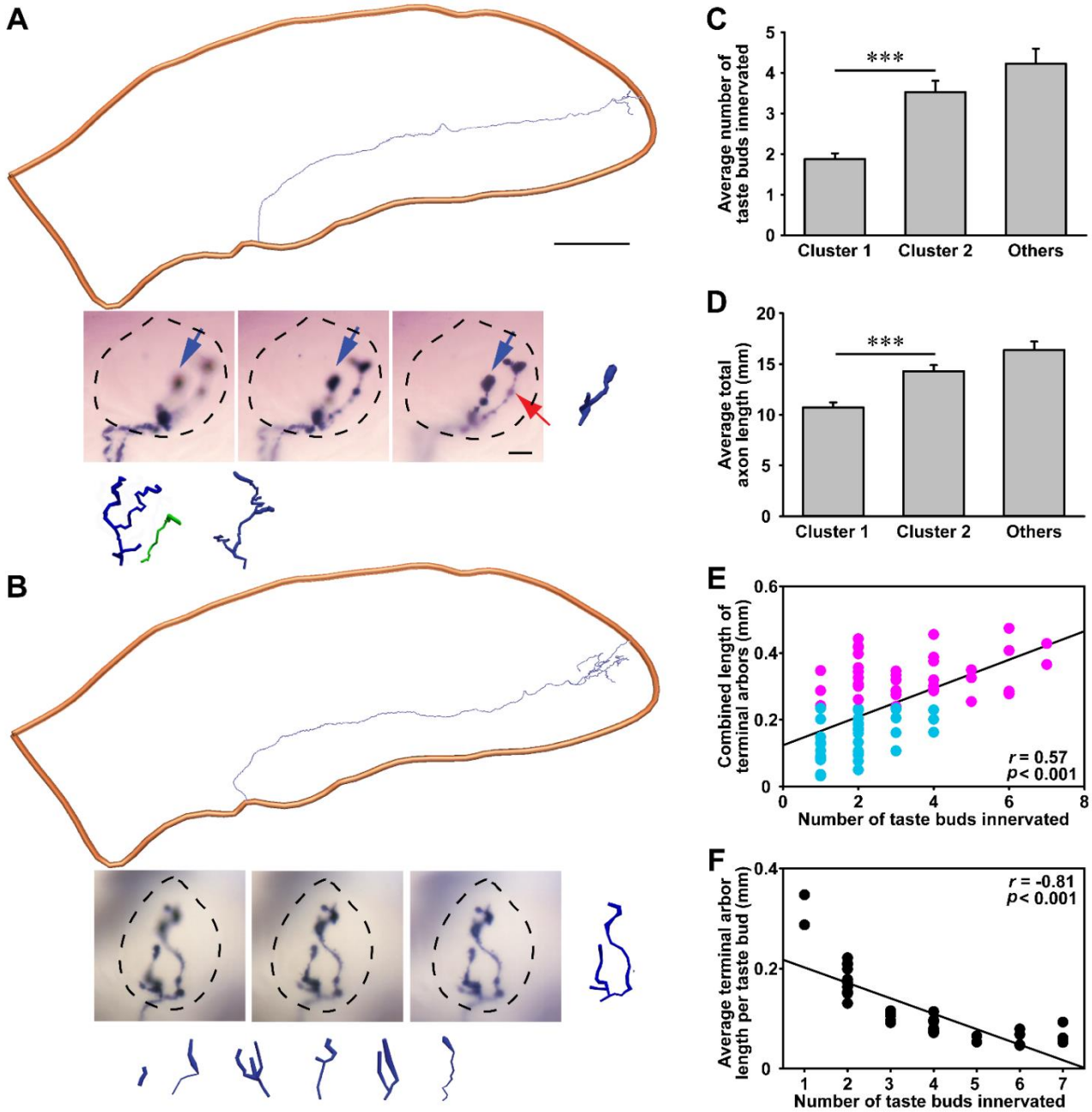

Figure 6. Two examples of the axons of cluster 2 neurons. (A) The 13.0 mm axon of this cluster 2 neuron had 3 branch points outside the taste bud producing 4 terminal arbors that innervated 3 taste buds (second arbor in same taste bud is green). Inside the taste bud some of the arbors branch further (5 branch points) to produce 9 branch ends. The imaged taste bud has a single arbor (blue arrow) from the reconstructed neuron plus one arbor from another labeled neuron (red arrow). (B) The 14.7 mm axon from the second neuron had 6 branch points below the epithelia, producing 7 terminal arbors, each of which innervated a separate taste bud. Some of these arbors also branched in the taste bud (6 branch points) resulting in a total of 13 terminal branch ends. (C) Cluster 2 neurons innervated significantly more taste buds than cluster 1 neurons. There was no significant difference between the numbers of taste buds innervated by cluster 2 neurons and clusters 3 and 4 neurons. (D) Similarly, the average total length of axons from cluster 2 neurons was significantly greater than the axons from cluster 1 neurons, but not different from neurons in clusters 3 and 4. (E) The more taste buds a neuron innervated the greater the combined total length of the terminal arbors (cyan=cluster 1, magenta=cluster 2). However, the cluster 2 neurons that innervated relatively few taste buds (1-3), have a much larger combined terminal arbor length than cluster 1 neurons. (F) The average length of the terminal arbors per taste bud was greater for cluster 2 neurons innervating a small number of taste buds and decreased as more taste buds are innervated. Black line indicates linear fit. ***P<0.001. Scale bars: 1 mm for whole nerve tracings in A and B; 10 µm for taste bud images and reconstructions within taste buds in A and B.

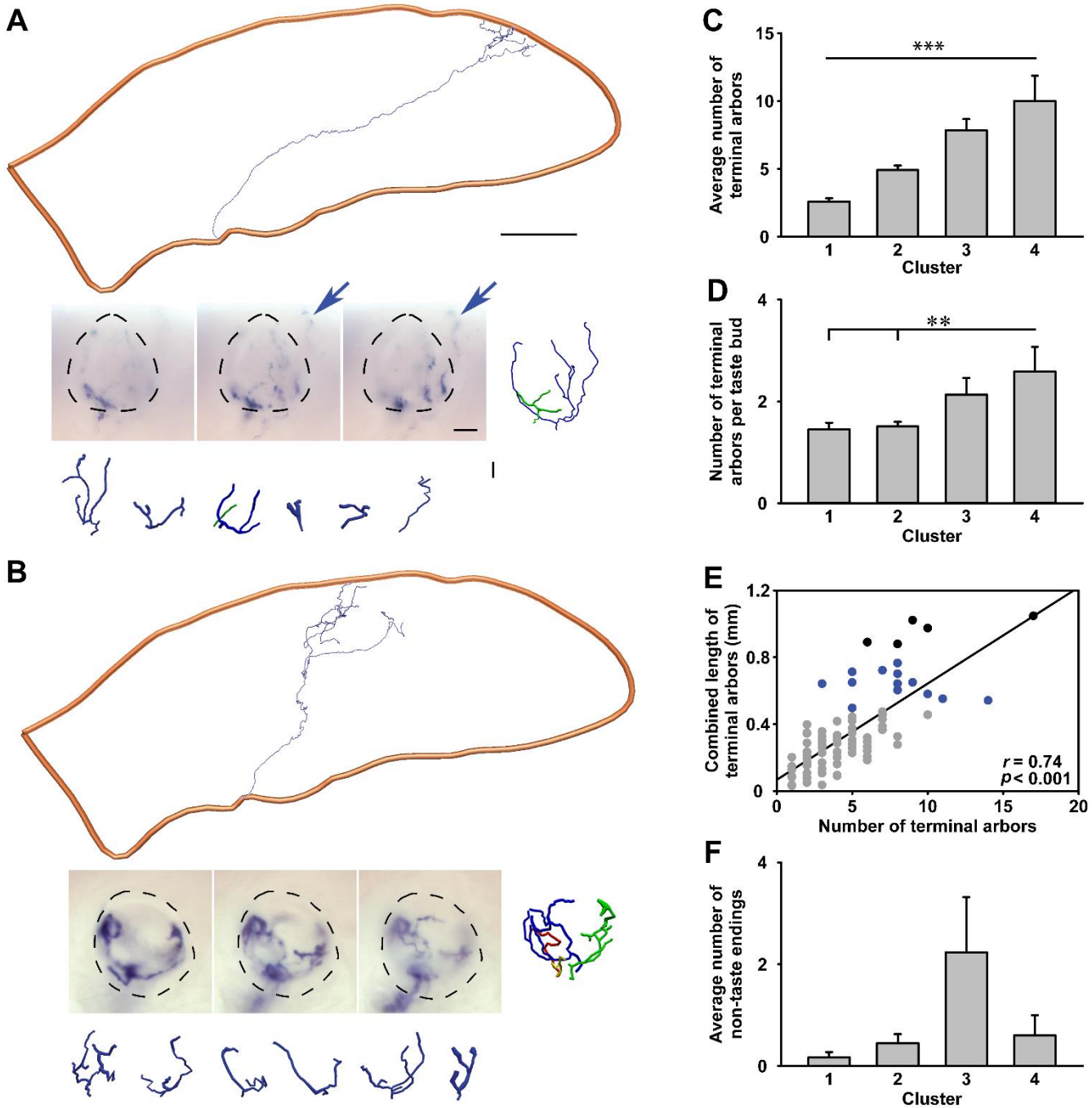

Figure 7. Two examples of cluster 3/4 taste axons. Images below each tracing show the AP staining of one taste bud innervated by a terminal arbor and the tracings of the other terminal arbors for this particular neuron. (A) The representative axon of a cluster 3 neuron had a total length of 18.6 mm, innervated 7 taste buds with 9 terminal arbors, and had 28 branch ends within the taste buds. For the two taste buds with two arbors the second one is shown in green. This axon also had an arbor branch innervating the epithelium outside of the taste bud (blue arrow, non-taste ending). (B) The axon of a cluster 4 neuron had a total length of 20.8 mm, innervated 7 taste buds, and had 10 terminal arbors with total of 40 branch ends. For this example, the imaged taste bud had 4 terminal arbors (dark blue, green, red, yellow). (C) The axons of cluster 3 and 4 neurons have more terminal arbors than those in clusters 1 and 2. (D) For the axons of cluster 3 and 4 neurons, the increase in terminal arbor number is due to an increase in the average number of terminal arbors innervating each taste bud. (E) Across all neurons, the best indicator of the combined terminal arbor length inside the taste bud is the number of terminal arbors (blue=cluster 3, black=cluster 4, gray = other clusters). (F) In addition, a subset of neurons in each cluster had axons terminating outside of taste buds (non-taste endings). Scale bars: 1 mm for whole nerve tracings in A and B; 10 µm for taste bud images and reconstructions within taste buds in A and B.

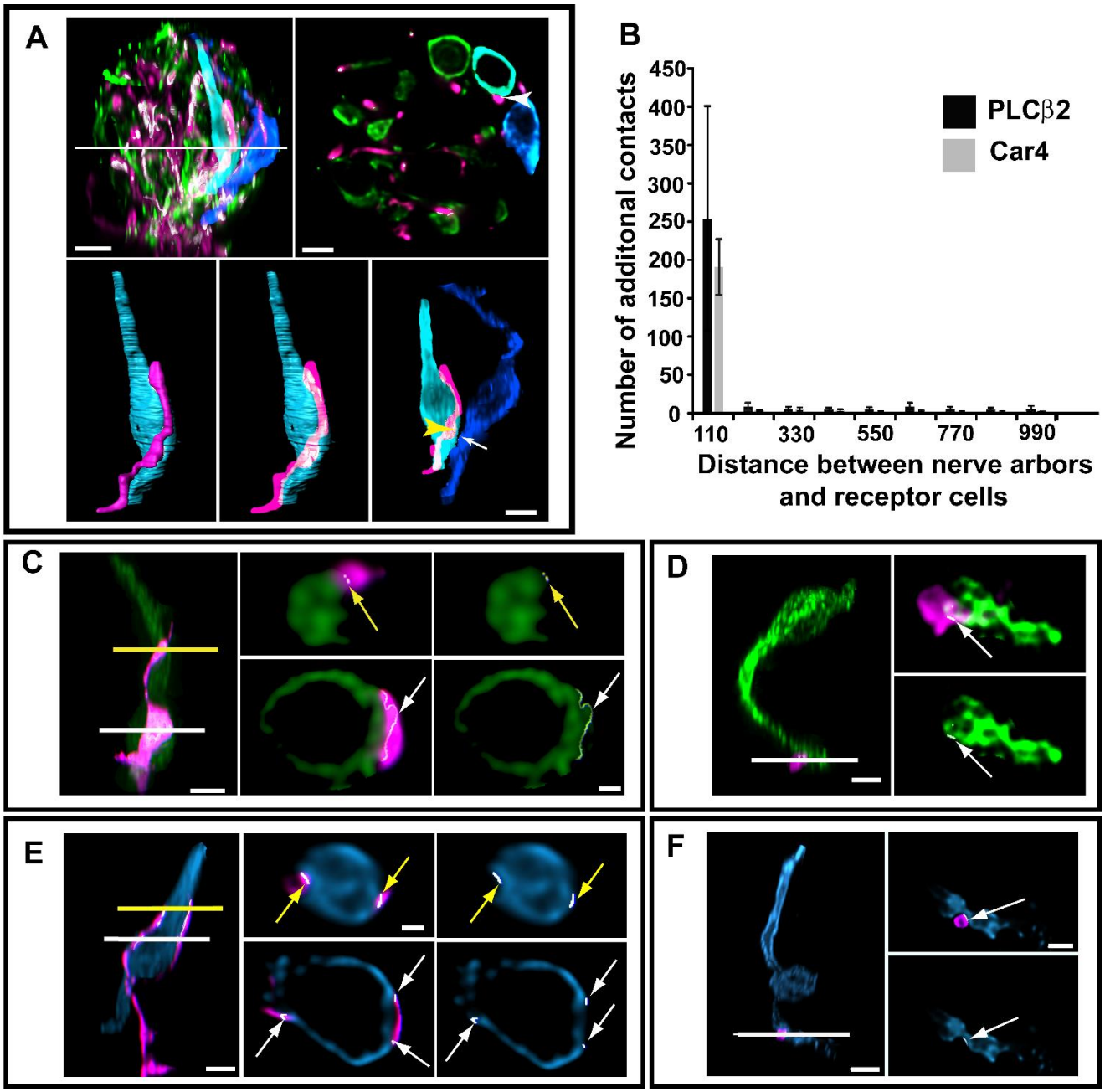

Figure 8. Determining the number of receptor cells contacting individual arbors. (A) A taste bud with all of the terminal arbors from taste neurons labeled magenta (tdTomato) and taste receptor cells expressing PLCβ2 labeled green (sweet-, bitter-, and umami-sensitive receptor cells), with example cells pseudo-colored teal or blue. The distance between nerve arbors and receptor cells was measured incrementally in 1.5 voxels (110 nm). Because the images were sampled at roughly twice the resolution of the light microscope, structures within 1–2 voxels cannot be distinguished as separate and often appeared as overlapping. These regions were pseudo-colored white. A single section through the taste bud indicated by the white line is shown to the right of the taste bud. A single magenta arbor (yellow arrowhead) contacts one PLCβ2-positive receptor cell (pseudo-colored purple). The next closest PLCβ2-positive cell to the same arbor was pseudo-colored teal is 1.2µm away (white arrow). (A, bottom) Three-dimensional reconstructions illustrate how by segmenting the cells and arbors and removing florescent outside the reconstruction and then removing the reconstruction permits the relationship between individual arbors and receptor cells to be viewed. (B) The axons of taste neurons have numerous locations where they are within a single voxel of a receptor cell. However, increasing the distance does not increase the number of additional contacts with new cells indicating that cells nerve fibers tend to be either within 200nm or greater than 1µm apart. This allowed us to set an objective criterion for this relationship. Scale bar in A=5µm, Scale Bar in B=3 µm and applies to B, D, E, F. This quantification was performed for all labeled nerve arbors and labeled taste receptor cells in six taste buds (labeled with either PLCβ2 [*n*=3] or Car4 [*n*=3]). (C, E) Some arbors extending along a nerve cell for a distance greater than 12 µm, others arbors contact cells for

shorter distances (D, F). Arbors tend to contact PLCβ2-labeled receptor cells (green) at widened regions of the arbor (C, D white arrows). Arbors tend to contact Car4-positive cells (blue) at sites of indentation of the nerve fiber into the cell (E, F, arrows). The fluorescence for each fluorophore was optimized for brightness contrast. For all panel's complete arbors and contacted receptor cells were segmented and the fluorescence outside the reconstruction removed, as illustrated in panel A. The reconstruction was removed and the fluorescence inside the reconstruction is what is shown in each panel.

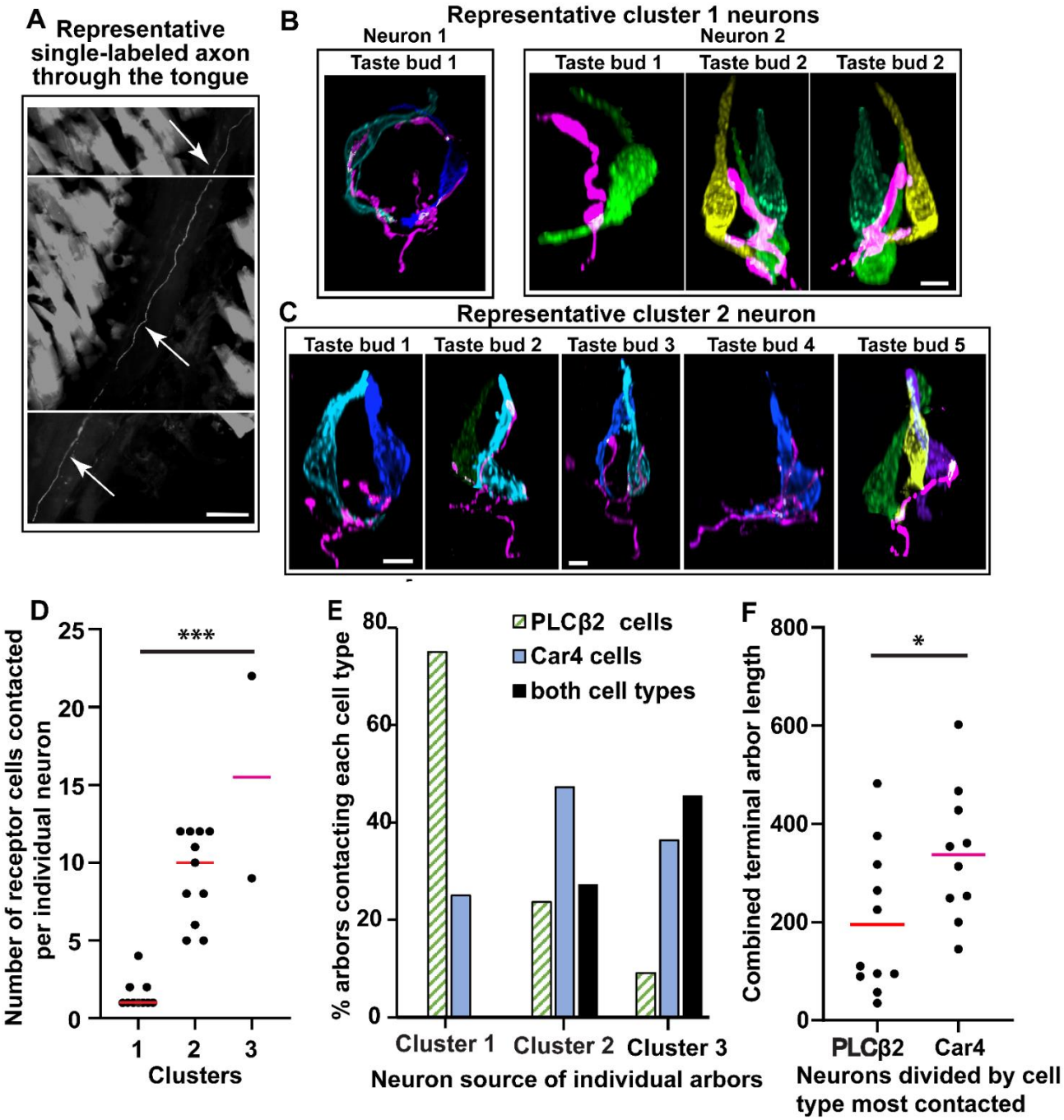

Figure 9. (A) A single axon is shown in three serial sections of tongue muscle (arrows). Scale bar = 50 µm. (B) Two cluster 1 neurons. One (left) innervates a single taste bud with one arbor that contacts two Car4-positive receptor cells. The second axon innervates two taste buds and contacts a total of four PLCβ2-positive receptor cells. The taste bud with 3 labeled PLCβ2 cells is shown in two different angles. (C) One cluster 2 neuron innervating five taste buds is shown along with the 10 receptor cells contacted. All scale bars = 5 µm. For all panel's complete arbors and contacted receptor cells were segmented and the fluorescence outside the reconstruction removed, as illustrated in Fig. 8A. The fluorescence inside the reconstruction is what is illustrated. (D) The numbers of receptor cells contacted by 21 single taste axons increases across cluster ($H_{(2,20)}$ =17.76;***p=0.0002). (E) Patterns are different in the number of arbors contacting each cell type across cluster 1 (χ^2 = 3.53; *P*=0.036), suggesting that neuron type/s likely differ across clusters. (F) When neurons are divided into groups based of the number of cells contacted, these two groups have different (t=2.28, p=0.34) but overlapping distributions of combined arbor length, suggesting that neurons contacting more Car4 receptor cells (sour transducing) are also more heavily branched.